Optimization model for the operation of a hydrogen production and storage plant powered by renewable wind energy

Daniel Filipe Santos da Costa Andrade

U. PORTO

FEUP **FACULDADE DE ENGENHARIA**
UNIVERSIDADE DO PORTO

Optimization model for the operation of a hydrogen production and storage plant powered by renewable wind energy

Daniel Filipe Santos da Costa Andrade

Mestrado em Engenharia Mecânica

September, 2023

Resumo

Esta dissertação tem como objetivo analisar a promissora intersecção entre a energia eólica e a produção de hidrogénio, como uma solução sustentável para o armazenamento e gestão de energia. Ao aproveitar o poder do vento para gerar eletricidade e convertê-la em hidrogénio, é possível desbloquear um potencial de armazenamento de energia eficiente produzido através de energia renovável.

Em primeiro lugar, uma compreensão abrangente do atual panorama da energia eólica, a nível mundial, assim como a nível nacional, será conduzida, de modo a introduzir o atual paradigma desta fonte de energia renovável. Posteriormente, todos os aspectos que influenciam a produção de energia eólica serão apresentados e avaliados, de modo a perceber como estes fatores influênciam a sua produção. Posteriormente, as propriedades inerentes ao hidrogénio como vetor energético e meio de armazenamento são apresentadas, assim como as várias tecnologias utlizadas para a sua produção.

Um dos contributos notáveis associado a esta tese prende-se com a realização de um exame aprofundado aos modelos matemáticos, que regem o comportamento e a interação entre estes dois sistemas, que posteriormente irão permitir a aplicação de técnicas analíticas e de considerações práticas, que governam todo o processo de investigação.

Através da utilização dos métodos acima estabelecidos, a análise do estudo de casos práticos, que servem como exemplos da eficácia do modelo no mundo real, permitem o estudo da viabilidade e da exequibilidade da utilização do hidrogénio como meio de armazenamento de energia. O primeiro caso de estudo investigou a viabilidade da utilização de hidrogénio como meio de armazenamento de energia em sistemas que têm como base a energia eólica, o que acabou por revelar uma certa imaturidade deste tipo de solução, no panorama atual. O segundo caso ofereceu uma solução para maximizar os lucros ao longo do tempo de vida de um sistema de produção de hidrogénio, o que permitiu calcular a dimensão óptima do eletrolisador, para um dado preço de venda hidrogénio, apelando à forma como estes sistemas poderão tornar-se cada vez mais atrativos economicamente. Posteriormente, esta investigação também contribuiu para a apresentação de soluções que integram o uso de energia sustentável, oferecendo casos práticos com o intuito de melhorar a eficiência energética e a viabilidade económica destes sistemas.

Ao enfatizar o uso de fontes de energia renováveis e o armazenamento energético a hidrogénio, esta dissertação procura contribuir para a temática relacionada com as preocupações ambientais contribuindo para um futuro energético menos poluente e mais sustentável. Em suma, esta tese de mestrado apresenta uma abordagem inovadora para satisfazer a crescente procura por soluções que recorrem a hidrogénio verde, contribuindo, deste modo, para o crescimento energias renováveis e para uma eficiente gestão da energia.

Abstract

This dissertation aims to analyse the promising intersection between wind energy and hydrogen production as a sustainable solution for energy storage and management. By harnessing the power of the wind to generate electricity and convert it into hydrogen, it is possible to unlock the potential for efficient energy storage produced through renewable energy.

Firstly, a comprehensive understanding of the current wind energy landscape at a global level, as well as at a national level, will be conducted in order to introduce the current paradigm of this renewable energy source. Subsequently, all the aspects that influence the production of wind energy will be presented and evaluated, in order to understand how these factors influence its production. Subsequently, the inherent properties of hydrogen as an energy vector and storage medium will be presented, as well as the various technologies used to produce it.

One of the notable contributions associated with this thesis is the in-depth examination of the mathematical models that govern the behaviour and interaction between these two systems, which will subsequently enable the application of analytical techniques and practical considerations that govern the entire research process.

Through the use of the methods set out above, the analysis of practical case studies, which serve as examples of the model's effectiveness in the real world, allow for the study of the viability and feasibility of using hydrogen as a means of energy storage. The first case study investigated the feasibility of utilizing hydrogen as an energy storage medium in wind energy systems, that revealed a present immaturity of this type of solution. The second case offered a solution to maximize profits over the system's lifetime by selecting the optimal electrolyser size for a fixed hydrogen selling price, these systems can become more economically appealing. Subsequently, this research contributed to the presentation of solutions that integrate the use of sustainable energy, offering practical cases with the aim of improving the energy efficiency and economic viability of these systems.

By emphasising the use of renewable energy sources and hydrogen energy storage, this dissertation seeks to contribute to the issue of environmental concerns, contributing to a less polluting and more sustainable energy future. In short, this master's thesis presents an innovative approach to satisfy the growing demand for solutions that use green hydrogen, thus contributing to the growth of renewable energies and efficient energy management.

Agradecimentos

Primeiramente gostaria de agradecer à minha família, mais concretamente aos meus pais por todo o apoio que me foi dado, não só para a escrita desta dissertação, mas nesta jornada que foi todo o meu percurso escolar até hoje. Deste modo, quero salientar todos os esforços, todos os sacrifícios, e todas a confiança que depositiram em mim, sem os quais eu nunca teria sido capaz de atingir tudo o que alcancei.

Um obrigado especial a todos os meus amigos pelo apoio incondicional que obtive, pela preocupação que sempre tiveram comigo e com o meu trabalho e por todos os momentos de descontração.

Um abraço enorme ao meu grupo da faculdade, por todos os momentos que vivemos nestes últimos cinco anos, o que é algo que sempre vou levar comigo nas minhas memórias.

Agradeço também ao meu orientador, o professor Eliseu Monteiro, por todo o apoio, todas as sugestões e por toda a disponibilidade que demonstrou.

Finalmente, não poderia deixar de agradecer ao grupo EQS Global pela oportunidade de elaborar a dissertação no seu meio laboral e por todos os almoços e atividades que realizamos. Agradeço, também, ao engenheiro Hugo Branquinho por esta possibilidade e ao engenheiro José Ferrão por todo o tempo que dispôs a guiar-me ao longo deste trabalho, por todos os conselhos dados e pela sua prestatividade.

"Sometimes I'll start a sentence and I don't even know where it's going. I just hope I find it along the way."

Michael Scott

Contents

List of Figures

List of Tables

Abbreviations and Symbols

AEL	Alkaline Electrolyzer
AFC	Alkaline Fuel Cell
AC	Alternating Current
AEP	Annual Energy Production
CHP	Combined Heat and Power
CO_2	Carbon Dioxide
DC	Direct Current
GHG	Greenhouse Gas
HVAC	High-voltage Alternating Current
HVAD	High-voltage Direct Current
HAWT	Horizontal Axis Wind Turbines
HST	Hydrogen Storage Tank
IPCC	International Panel on Climate Change
MCFC	Molten Carbonate Fuel Cell
MERRA-2	Modern-Era Retrospective analysis for Research and Applications, Version 2
MILP	Mixed Integer Linear Program
OM	Operation and Maintenance
PNEC	National Climate and Energy Plan
PAFC	Phosphoric Acid Fuel Cell
PEM	Polymer Electrolyte Membrane
PEMEL	Proton Exchange Membrane Electrolyzers
PV	Photovoltaic System
ROI	Return On Investment
RPM	Rotations per Minute
SOFC	Solid Oxide Fuel Cell
SOE	Solid Oxide Electrolyzer
STEPS	Stated Policies Scenario
VAWT	Vertical Axis Wind Turbines
WEO	World Energy Outlook
WT	Wind Turbine
YSZ	Yttria-stabilized Zirconia

Chapter 1

Introduction

Electric energy is a form of kinetic energy that results from the flow of electric charge. Thus, this energy is generated when electrons are made to flow from one place to another. The movement of these electrons are employed through a conductor and, for that purpose, a copper conductor wire is used. For this purpose, energy can be obtained through different alternatives such as fossil fuels, nuclear power and renewable resources.

Fossil fuels, mainly coal, oil and natural gas, are the most widely used source of energy production in the world. They are burned to produce thermal energy, which is then converted into mechanical energy and then into electrical energy through turbines and generators. Fossil fuels are known to have finite reserves and are predicted to deplete within the next decades if they continue to be exploited at the current pace. This factor allied with the accumulation of CO_2 in the lower layers of the atmosphere gives way to climate change, floods, intensive rainfalls and droughts. These are the main motives that caused the present search for clean, sustainable, and environmentally friendly alternative energy sources. In order to complete a transition to a cleaner and safer environment, it is necessary to replace the energy obtained from fossil fuels with renewable alternatives such as wind, solar and other energy sources.

On the other hand, renewable energy sources include solar, wind, hydro, geothermal, and biomass energy. These sources of energy a more sustainable and environmentally friendly option since they do not produce greenhouse gases (GHG) emissions, such as carbon dioxide. This type of energy can be produced using solar panels, wind turbines, hydroelectric dams, geothermal power plants, or bioenergy systems.

Another alternative regarding energy production is the nuclear energy. This energy is generated in a nuclear power facility containing nuclear reactors, which releases large amounts of thermal energy used to produce steam and generate electricity through turbines and generators.

The current paradigm on the planet is focused on two aspects, one is the climate change, since it is the major threat to the future of humanity, with extreme climatological and meteorological events escalating in frequency and intensity. The global temperature has increased by $1.2\,°C$ since pre-industrial times (before 1850) and it is not slowing down since it is projected to rise $1.5\,°C$ within 15 to 20 years if GHG emissions are not drastically reduced. The increase in temperature

is mainly due to the world's increased use of fossil fuels and deforestation. The United Nation's International Panel on Climate Change (IPCC) warns that exceeding a 1.5 °C temperature increase will be catastrophic.[38] Therefore, in order to prevent this crisis, the organization mentioned suggests that by 2030 the CO_2 emissions must be reduced by 45% over the 2010 levels in order to ultimately reach net zero by 2050. To achieve this goal, the world economy would require rapid and widespread changes in energy use, land use, transport, industry, agriculture, and construction by focusing on obtaining energy from renewable sources and enhancing energy efficiency. However, persistent growth in the human population requires an ever-increasing consumption of energy and natural resources, nullifying gains made from efficiency improvements in resource use and expansion of renewable energy production. At the present rate of use, fossil fuels will be critically depleted within 50 years.[27]

Another key aspect of the contemporary worldview paradigm is the global energy crisis that is currently occurring, caused by to Russia's invasion of Ukraine. This conflict has led to supply shortages and higher energy bills, particularly in gas markets, due to Russia's curtailment of natural gas supply to Europe. This factor caused the acceleration of the transition to clean energy, leading to new policies and investments in major markets, that increased clean energy investment with the aim of to cutting GHG emissions more rapidly and bring electricity costs down. With this investment, there will be an continuous increment in renewable electricity generation that will allow the decline of the share of fossil fuels in total electricity production, leading to a more sustainable energy production system.

The World Energy Outlook (WEO) also reveals that at the current growth rate for deployment of solar PV, wind, EVs (electric vehicles), and batteries would lead to a faster energy transformation than projected in the Stated Policies Scenario (STEPS) that were explored in the WEO. In the case of electrolysers for hydrogen production, the potential excess capacity of all announced projects relative to the 2030 outlook is around 50%.[10]

1.1   Project Description

The outline of this thesis is centered around the production of hydrogen from wind energy and its utility as an energy storage medium. To achieve this objective, the thesis begins with an introduction to the current global and Portuguese wind energy landscape. It also delves into the various aspects involved in the generation of wind energy.

The thesis proceeds to explore hydrogen in detail, providing insights into its properties and the methods employed for its production. This section also includes a comprehensive characterization of various electrolyser and fuel cell technologies available for hydrogen production and utilization.

Following the introduction of the key concepts and methodologies, following some considerations make and also the mathematical model behind this analysis, this thesis conducted an in-depth examination of two practical case studies to demonstrate the real-world applicability of the proposed methods.

The first case study aimed to assess the feasibility and practicality of utilizing hydrogen as an energy storage medium. This analysis involved an evaluation of the entire process, from wind energy generation to hydrogen production and subsequent reconversion into power.

The second case study further explored the economic aspects of an hydrogen generation system, considering factors such as return on investment, profit generation, and the influence of variables such as hydrogen selling prices and electrolyser capacities on financial outcomes.

By conducting these case studies, the thesis aimed to provide practical insights into the potential of integrating wind energy and hydrogen production as a sustainable energy storage and utilization solution. The findings and recommendations derived from these case studies contribute to a deeper understanding of the real-world applications of this innovative approach.

1.2 Thesis Structure

Chapter 1 is the opening chapter of this thesis that serves as an introduction to the research and it includes two sections:

Section 1.1 provides an in-depth overview of the project's nature, scope, and objectives. It discusses the background and motivations that led to the undertaking of this research and section 1.2 to offer clarity and guidance to the reader, this section outlines the structure and organization of the thesis, providing an overview of what to expect in each chapter and section.

Chapter 2 constitutes a comprehensive literature review, where key topics relevant to the research are explored and analyzed. This chapter is further divided into several sections:

Section 2.1.1 delves into the realm of wind energy, discussing its global significance. It explores the state of wind energy in both the world and Portugal, highlighting its challenges. The section also examines wind turbine components, classifications, wind characteristics, and the process of wind power conversion. Section 2.2 shifts the focus to hydrogen, this section covers various aspects related to its production. It explores different methods of hydrogen production, with a particular emphasis on water electrolysis. Subsequently, section 2.3 delves into the aspects of hydrogen storage and distribution. Concluding this chapter, section 2.4 provides an overview of fuel cells, a important component in the research.

Chapter 3 outlines the methodology employed in the research and it starts with:

The mathematical modeling in section 3.1 that discusses the mathematical models utilized in the study, including models for both wind farms and hydrogen systems. In order to present the tools, software, and resources selected for the analysis, section 3.2 is employed.

Chapter 4 presents two case studies that serves as a practical application of the research methodology, comprising the following sections:

Section 4.1 introduce some wind and fuel cell projects that are currently in progress at a worldwide level. Afterwards, the specific problems addressed within the case study are outlined in section 4.2. Section 4.3 present an analysis on detailed wind data collected at the site and consequent wind power production. With this information, the first case is present in section 4.4, focusing on hydrogen as an energy storage solution utilizing fuel cells to meet the power demand that was

previously defined. In order to conduct an economic evaluation of a hydrogen production system, The second case study is explored, in section 4.5.

Finally in Chapter 5, the thesis presents its conclusions, summarizing the key findings and insights derived from the research conducted throughout the study. Additionally, in section 5.1, the thesis outlines potential future research directions, offering suggestions for further investigation and expansion of the knowledge in the field of hydrogen production and its applications.

Chapter 2

Literature Review

2.1 Wind Energy

"Wind energy is delivering more clean power to Europe than ever before – meeting 17% of its electricity demand in 2022, up from 13% five years ago. And the further build-out of wind will be key to reducing our dependence on imported fossil fuels and transitioning to climate neutrality."

Sven Utermöhlen CEO,

RWE Offshore Wind WindEurope Chairman

Wind results from the movement of air due to atmospheric pressure gradients as the air moves from high-pressure areas to low-pressure areas causing the phenomena denominated by wind. The larger the atmospheric pressure gradient, the higher the wind speed and thus, the greater the wind power that can be captured from the wind by means of wind energy-converting technology. The generation and flow of wind are processes influenced by a numerous factors. These factors include the Coriolis effect, which results from the Earth's rotation, variations in solar heating, and local geographical conditions.

Wind energy is a dominant energy source for new power generation and it has a great impact in the global energy market. The technical maturity of wind power, its rapid deployment, and the fact that there is no practical upper limit to the percentage of wind that can be integrated into the electricity system make it a leading energy technology.

As an inexhaustible and free energy source, it is available and plentiful in most regions of the earth. Additionally, greater use of wind energy would contribute to a decrease in the need for fossil fuels, which, based on current consumption, may become scarce at some point this century. In addition, wind energy is significantly less expensive per Kilowatt hour (kWh) than solar energy. Thus, it is anticipated that wind energy, the most promising energy source, will be crucial to the world's power supply in the twenty-first century.[48]

2.1.1 Wind Energy in the World and Portugal

New wind installations in Europe totalled 19.2 GW of produced power in 2022, represented by 2.5 GW offshore wind capacity and 16.7 GW produced onshore. This year was particularly important for installations in Europe due the 4% grow in wind power generation when compared to the previous year, despite the difficult economic, climate and supply chain issues. Installations, however, were 12% below the realistic expectations scenario for 2021 and significantly below the rates necessary to achieve Europe's climate and environmental objectives. By 2030, the annual average wind energy production should increase 31 GW in order for the European Union to reach its predictions and the goal of 45% of the energy to be from renewable sources.[13] The growth achieved in this year was 55% higher than the one reached in 2020 leading to the highest growth among all renewable power technologies. Wind remains the leading non-hydro renewable technology in the world, generating 1870 TWh in 2021, almost as much as all the others combined.[8] In Europe, the amount of wind energy produced has increased gradually from 370 TWh in 2018 to 489 TWh in 2022, with the exception of one unusual year in 2021 when production was lower than in 2020. In the same time frame, the demand for energy decreased from 2960 TWh in 2018 to 2830 TWh in 2022. This decline was mainly due to the lockdown caused by the COVID-19 pandemic in 2020 and the conflict in Ukraine in 2022.[13]

	Germany	Spain	UK	France	Sweden	Turkey	Italy	Nether-lands	Poland	Denmark	Portugal	Finland	Belgium	Norway	Others
Onshore	58	30	15	21	14	12	12	6	8	5	6	6	3	5	25
Offshore	8	0	14	0	0	0	0	3	0	2	0	0	2	0	0
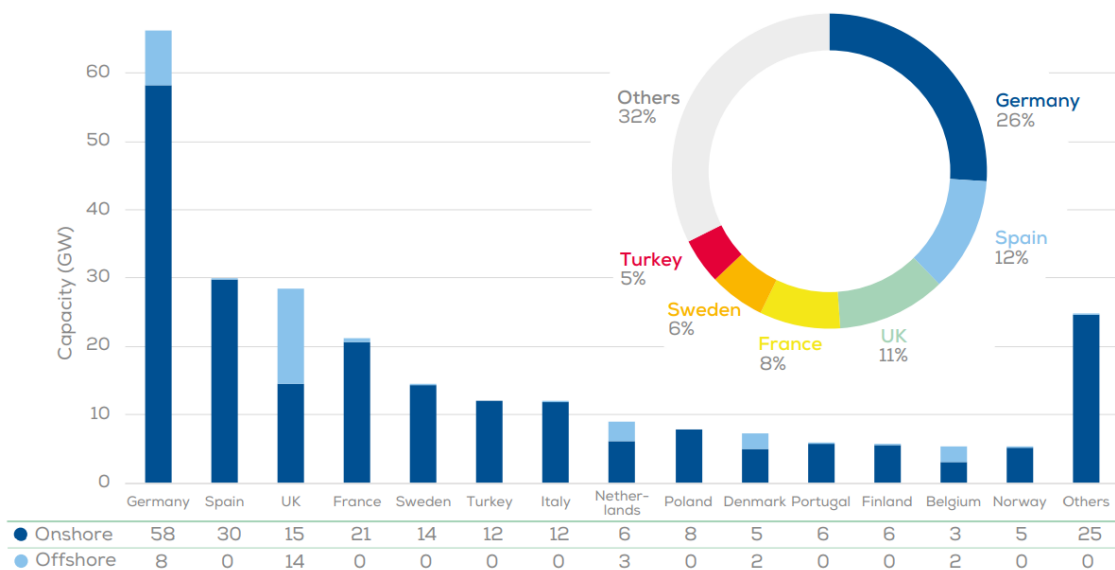
Figure 2.1: Total wind power installed capacity the European Union in 2022[13]

Portugal has developed its own National Climate and Energy Plan (PNEC 2030) within the framework of EU directives, which sets a higher goal of a 47% share of renewable energy sources in its total electricity usage by 2030.[7] Portugal is one of the EU member nations best positioned to meet the 2030 targets. The consumption of energy, in this country, was 50.78 TWh of electricity in 2020, making renewable energy account for 34% of gross final energy usage, placing it ninth, among EU nations in this category. However, 18.91 TWh of energy was generated using fossil fuels, and only about 3% of the total electricity consumed was imported from other countries.

Therefore, there is still much work to be done to meet the PNEC 2030 goal.[25] From a European point of view, Portugal is the fourth-biggest wind power producer since the share of wind energy in all the installed capacity is 26% corresponding to a total of 90 MW of onshore energy produced in 2023 that is excepted to increase to 380 MW in 2027.[13]
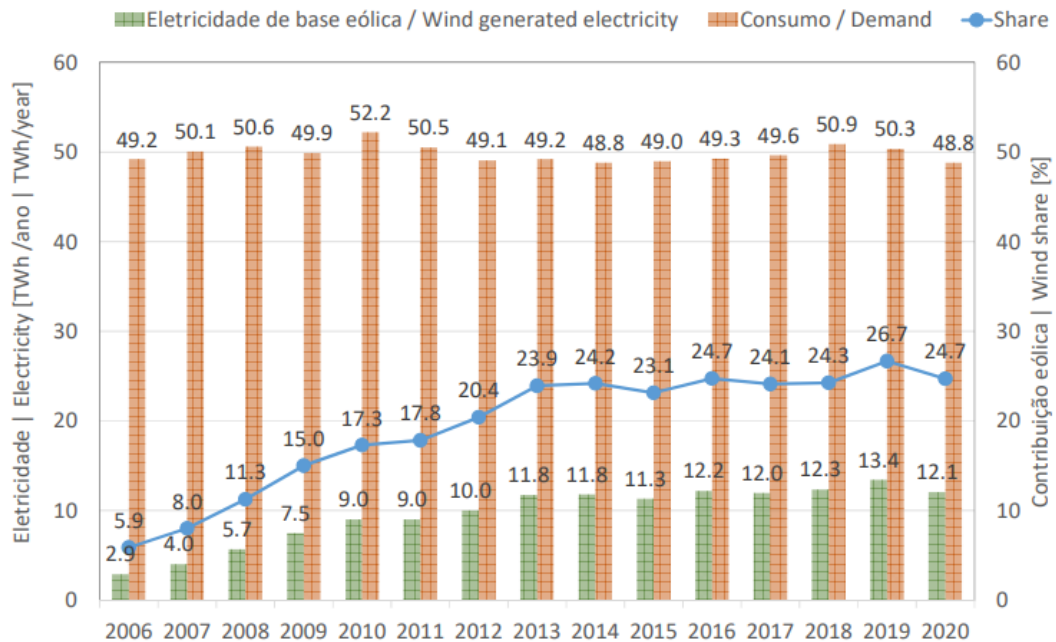
Figure 2.2: Wind generation vs Eletricity demand 2006-2020 in Portugal's mainland.[28]

At a practical overview, it is important to underline a state-of-the-art project in Viana do Castelo, Portugal, that combined the production of green hydrogen with wind electricity. The WindFloat Atlantic wind farm was one of the first to use a semi-submersible platform for industrial wind farm deployment. It was put into service in 2020 and consists on three 8.4 MW turbines that are sustained by a semi-submersible structure made of three cylinder buoys spaced 50 meters apart and 30 meters high. Some advantages of this design are an unobstructed area of 1082 m ^{2} due to the simple assembly of the wind turbine on the structure in port and hydrogen production by individual electrolysers.[23]

2.1.2 Wind Energy Challenges

The proper design of wind turbines is a critical challenge that involves considering blade loading and aerodynamic stability. Hence, several researchers have developed mathematical models to calculate material and structural stresses for improved horizontal axis and vertical axis wind turbine design. Methods such as multi-objective optimization, probability-based extreme-response determination, and adaptive neurofuzzy inference system analysis have been employed to enhance wind energy generation. The design parameter of the aerofoil shape plays a significant role in understanding the aerodynamics of the blade, and new aerofoils have been developed to improve wind turbine energy capture. Researchers have also focused on designing slender blades to increase lift

coefficient and reduce fatigue and extreme loading, resulting in higher lift-to-drag ratios. Modifications such as diffuser augmented wind turbines (DAFT) and building augmented wind turbines (BAWT) have been explored to enhance wind energy generation.[15]

Constructing wind energy farms requires securing large areas of land in rural areas with sufficient wind speeds. However, due to a number of variables, wind speed can fluctuate, making it difficult to deliver consistent electricity. To address this problem, power system regulators can be used to establish reserve capacity and create thorough schedule plans. Accurate forecasting methods, such as the two-parameter Weibull probability density function and machine learning techniques, have also been used to predict wind speed distribution and increase wind power penetration.[50] Wind farms are typically situated in rural regions because of the availability of land, higher wind speeds, and the possibility of other activities like farming. However, two significant problems arise in generating wind energy with respect to the grid. Firstly, in several rural areas, the grid infrastructure is inadequate to receive the power generated by the farm. Secondly, even if a stable grid is present, integrating wind energy into the grid can lead to potential technical issues such as voltage fluctuations due to the variations in wind energy.[15]

Regarding the environmental issues associated with the production of wind energy,two main aspects can be outlined. Noise pollution is the most critical environmental impact of wind turbine since its effect has the potential to lower property values within a varying radius of the construction. As a result, turbines should be set back from residences and property lines to insulate participating and neighboring landowners from noise and safety concerns. Before building a wind turbine, engineers must be familiar with the types of noise a wind turbine produce. Despite being the most compatible energy source with animals and human beings in the world, wind energy does have some reported impacts on wildlife. These impacts can be categorized as either direct or indirect. Direct impacts refer to mortality caused by collisions with wind energy plants, while indirect impacts include avoidance, habitat disruption, and displacement. However, it's worth noting that these impacts are relatively minor compared to those caused by other sources of energy. Additionally, researchers and industries are actively working to develop protections and preventions to further minimize the wildlife impacts associated with wind energy. [47]

Wind energy is a capital-intensive technology, with the majority of expenditures made at the time of investment, and initial expenditures can be as high as 80% of the total cost of the project. While wind energy is a cheap option, improper funding conditions during the initial phases can difficult the progress of the project. The production cost of wind energy is also relatively high due to the intermittent nature of wind and high investments. Thus, investors must consider whether there investment in wind is profitable or not, however wind power prices are decreasing steadily and wind power can offer a better return on investment over a long period of time. To minimize the production cost of wind energy, it is important to optimize wind power plant design, use power regulators and flexible AC transmission systems and also improve wind power forecasting accuracy. Although, naturally, resorting to these measures will incur additional costs.

High production costs are determined based on power produced and the fixed costs such as interest, land rent, insurance, and variable costs mainly due to the operation and maintenance of

the wind farm. It is not always possible to implement wind energy on a large scale due to the intermittent nature of wind at site and the high investment that would be nedeed to produce clean energy at that location. The production cost can be minimized by proper planning and taking necessary actions, such as increasing the wind power penetration, which will ultimately lead to more energy generation. To achieve this goal and to improve the consistency in wind power production it is necessary to resort to accurate forecasting methods. The use of power system regulators can make detailed schedule plans and set reserve capacity for proper utilization of energy. Overall, wind power prices are decreasing steadily nonetheless wind power can offer a positive return on investment over a long period of time. However, when investing in this technology investors must also consider the risk associated to it. [31]

2.1.3   Wind Turbine Components

Although modern wind turbines come in various sizes, they typically consist of several key components that can be classified as either mechanical or electrical components. The most visible parts are the tower, nacelle, rotor blades, and step-up transformer. The rest of the components are housed inside the wind turbine. The major components of a Wind Energy Conversion Systems (WECS) are broadly classified into three categories:

- **Mechanical Components**: Includes the rotor blades, rotor hub, rotor bearings, main shaft, mechanical brake, gearbox, pitch drives, yaw drives, wind measurement unit, nacelle, tower, foundation, heat exchange system, and ladder.

- **Electrical Components**: Includes the wind generator, power electronic converter along with generator- and grid-side harmonic filters, step-up transformer, power cables, wind farm collection point, and switch gear.

- **Control Components**: Includes mechanical and electrical-related control systems.

The rotor components include rotor blades, rotor hub, rotor bearings, nose cone, and pitch drive. The "drivetrain" includes mechanical coupling, bearings, low-speed main shaft, high-speed generator shaft, gearbox, and mechanical brakes. A brief description of the major mechanical components is given as follows. [60]

- **Rotor** - A rotor consists of large blades resembling an airplane wing, containing, typically, three blades for a turbine. [33] Rotor blades are air-foil shaped and the wind flows more quickly along the curved edge, creating a difference in pressure on either side of the blade. In order to equalize the pressure difference, the blades are "pushed" by the air allowing the blades to turn. [9]

- **Pitch and Yaw drives** - In situations with strong wind speeds, another component known as the "pitch drive" is used to lessen the impact of lift forces. This is required to ensure that the alternator operates at a pace that is consistent within a stable power system operation. [33]

The yaw drive is used to move the rotor blades and nacelle toward the wind to extract the maximum possible energy. The yaw drive is composed by electric motor drives, yaw gear, gear rim, and bearings and produces high torque to turn the nacelle. When the wind speed is above the cut-out value or when a malfunction occurs, the yaw mechanism helps stop the turbine by moving it out of the wind direction.[60]

- **Nacelle** – The nacelle contains a set of gears and a generator. The turning blades are linked to the generator by the gears. Since most generators require a speed of 1000–3600 RPM to generate electricity and the turbine rotor only produces a rotational speed of less than 100 RPM, gearboxes are usually integrated in this component in order to convert low rotor speed into higher speeds securing a correct generator functioning.[33] The generator then converts the rotational energy from the blades into electrical energy.[9]

- **Tower** – The tower is constructed to hold the rotor blades off the ground and at an ideal wind speed. Towers are usually between 50-100 m above the surface of the ground or water in order to achieve better speed, less turbulence and turmoil, and quantity of wind to the components mounted at its top such as the blades and the nacelle. Offshore towers are generally fixed to the bottom of the water body, although research is ongoing to develop a tower that floats on the surface.[9]

A controller, anemometer, heat exchanger and wind vane are additional crucial parts of a wind turbine as the heat exchanger cools the generator and the controller is a computer operated system that controls the turbine's operation.[33]

An anemometer and wind vane are key components, typically mounted on the top back part of the nacelle, that are responsible for the continuous wind data monitoring and extraction, indispensable for the pitch and yaw drives, as well as electrical control systems. Anemometers are used mainly to measure the wind speed and, for that purpose, are composed by a three-cup vertical-axis micro-turbine and a speed transducer. For a more accurate and reliable wind measure ultrasonic anemometers are used. Furthermore, a wind vane along with an optoelectronic angle transducer measures the wind direction.[60]

Subsequently, if the turbine in question is a direct drive turbine, the rotor connects directly to the generator otherwise this connection can be implemented through a shaft and a gearbox that will speed up the rotation and allow for a physically smaller generator. This translation of aerodynamic force to the generator's rotation creates electricity.[4]

Figure 2.3 represents all the components that were mentioned above that assembled together build up an complete wind turbine.
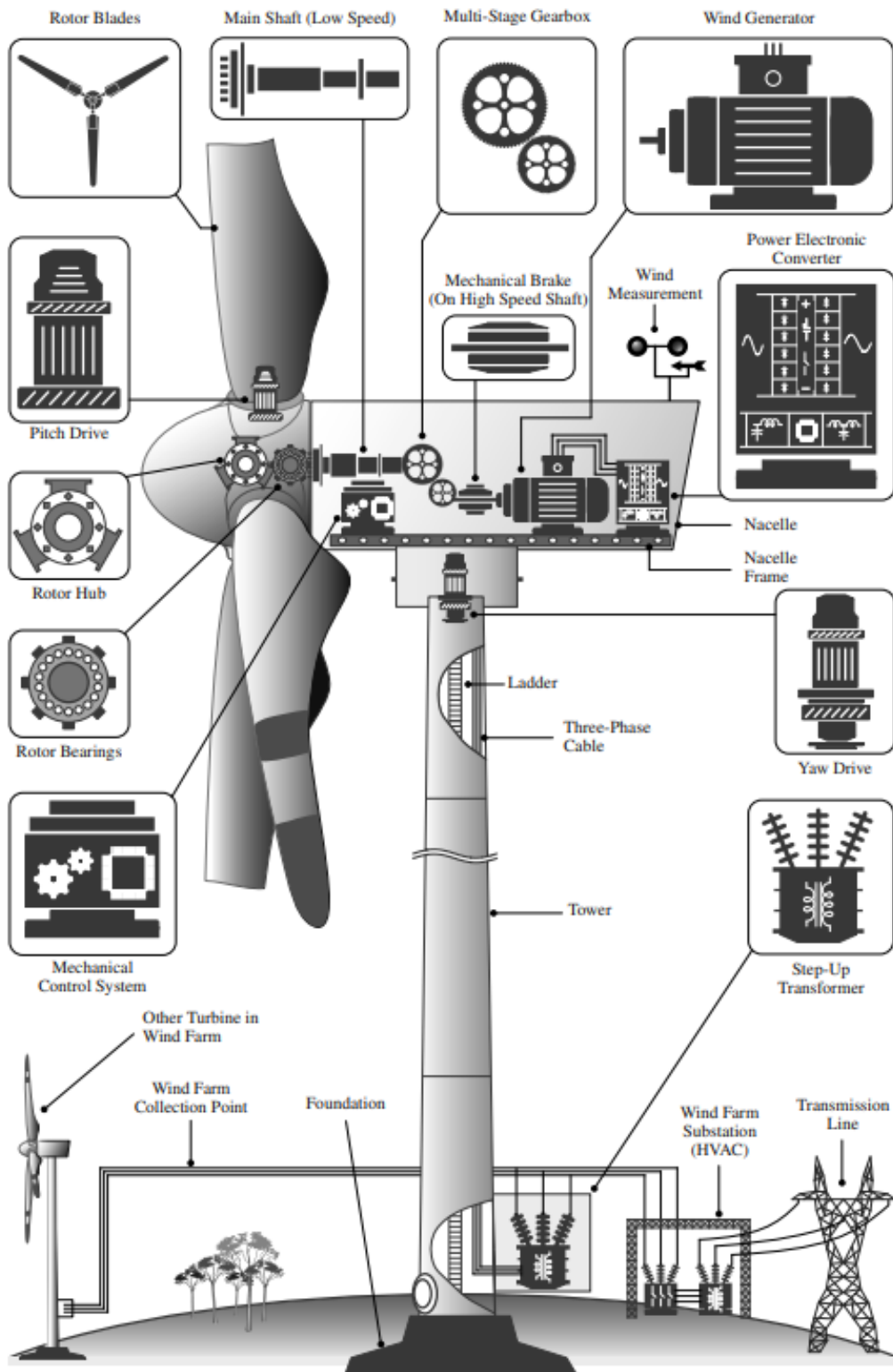
Figure 2.3: Illustration of a wind turbine's components.[60]

2.1.4 Wind Turbines Classifications

High-voltage alternating current (HVAC) or high-voltage direct current (HVDC) transmission lines are used to feed wind farm electricity into a grid. When choosing between HVAC and HVDC transmission, two essential factors need to consider such as the amount of power to be delivered and the distance between the wind farm and the local utility grid. HVAC transmission is more favorable for small-scale wind farms, which are situated near to the utility grid and HVDC transmission is a great option for power ratings and distances larger than 400 MW and 60 km, respectively.[60]

The design and size of a turbine play a crucial role in electricity generation. The recent trend is toward large turbines with longer blades that sweep wind from a larger area to increase the production of energy. Modern wind turbines can be divided into two types: horizontal axis wind turbines (HAWT) and vertical axis wind turbines (VAWT).

HAWT have blades that rotate around a horizontal axis and are the most commonly used type of wind turbine. They are efficient in generating high amounts of energy in areas with consistent wind patterns and are commonly used in commercial and utility-scale applications. However, they are often more expensive to install and maintain. These wind turbines can also be classified based on their rotor diameter into large, medium, domestic, mini, and micro scale turbines as labelled in Table 2.1.[41]

Technology type	Rotor diameter (m)	Rotor swept area (m^2)	Nominal power (kW)	Wind speed regions	Suitable applications
Large scale	50–100	1963–7854	> 1000	Very high	Large scale grid power generation (onshore and offshore wind farms)
Medium scale	20–50	314–1963	100–1000	High	Mini wind farms (smart/micro grid application in remote areas, village power)
Small scale	10–20	79–314	25–100	Good	Residential purpose, rural electrification, water pumping, and telecommunication sites
Domestic scale	3–10	7–79	1.4–16	Moderate	Hybrid systems

Table 2.1: Classification of HAWT[41]

VAWT have blades that rotate around a vertical axis and are considered mostly for small scale power generation, usually less than 100 kW. They are typically used in residential and urban environments, where wind patterns are less consistent and variable. The trend in the small wind

turbine market is toward isolated or off-grid applications such as rural electrification, mini wind farms, research and education, telecommunication stations, off-shore generation, and recreational boats. The International Electrotechnical Commission (IEC) has defined technical standards for small wind turbines, with a power rating of about 50 kW for turbines with rotor swept area of less than 200 m^2 and a generation voltage level of less than 1000 V AC or 1500 V DC. The small wind turbine market has grown steadily over the years, driven by the increasing demand for renewable energy sources and advancements in wind turbine technology. According to a report by the Global Wind Energy Council, the global installed capacity of small wind turbines reached 963 MW in 2019, with a growth rate of 13.8% compared to the previous year. The report also suggests that the small wind turbine market is expected to continue growing in the coming years due to increasing government support and incentives, technological advancements, and growing demand from residential and commercial sectors. There are currently 330 small wind turbine manufacturers around the world, with an additional 300 companies involved in marketing, consulting and services since the majority of these manufacturers are located in China, the USA, the UK, Canada, and Germany.[41]

While HAWT's dominate the market due to their greater efficiency and energy output since they require less space to generate the same amount of energy, VAWT's still have their share of advantages such as low noise levels, ability to capture wind from any direction, effectiveness in rooftop and small-scale applications as generally they are less expensive to install and maintain.[41][33]

Continuous research and advancement of turbine technology have taken place over the last several decades, resulting in a phenomenal development of wind energy technology. In the last few decades, significant advancements in technology have been made in areas such as the WT rotor size, tower heights, wind turbine dependability and efficiency and cost-effective wind turbine siting. With this development, a new generation of wind turbines such as Kite generation turbines and Magenn Air Rotor Systems (MARS) turbines arose, operating at altitudes between 183 and 305 m and 800-1000 m, respectively.[41]

Matching the site-specific wind circumstances with the model's design classification, which includes rotor size, tower heights, reliability and efficiency is the main consideration in the process of choosing a wind turbine, along with the evaluation of the wind turbine's price. Design configurations, operational mechanisms, and physical structure appearances such as axis orientation, aerodynamic forces, rotor location and speed, number of blades, transmission, power control, yaw orientation and hub type are also important variables to take into account. In addition, general commercial factors such as the analyst's familiarity with the models, the manufacturer's track record and reputation, the product's technological advantages, reasonable prices, and warranty terms need also to be taken into account.[34]

Relatively to the wind turbine's operating location, two alternatives arise since they can be sited onshore or offshore. Onshore wind turbines have a long history on its development and have a number of benefits, including less expensive foundations, simpler electrical grid integration, less expensive tower construction and turbine installation, and easier entry for maintenance and

operation. Due to the superior offshore wind resource in terms of wind intensity and continuity, offshore wind generators have advanced more quickly than onshore ones since the 1990s. A wind turbine installed offshore can make higher power output and operate more hours each year compared with the same turbine installed onshore. Furthermore, environmental regulations are more relaxed in offshore relatively to onshore sites. For offshore wind farms, for example, the noise emitted by the turbine is no longer a concern.[55]

2.1.5   Wind Characteristics

Wind velocity changes according to geographical location, hourly, seasonally, with the height above the earth's surface, and with weather and local orography. Understanding wind characteristics will aid in the optimization of wind turbine design, the development of wind measuring methods, and the selection of wind farm sites.

Wind speed is a useful measure for evaluating a region's potential for producing wind energy. Each region's weather condition can be modeled using statistical parameters of wind speed data. Through this model it is possible to evaluate wind turbine performance and thus, the technical, financial, and carbon footprint viability of wind energy production in a region. The wind speed profile can be modelled with various probability distribution functions including Weibull, Gamma, Rayleigh, and Log-Normal.[16] However, the Weibull distribution is the most widely used model in wind speed data analysis and thus it will be approached in the below section.

The amount of energy available in the wind at a given location is the average amount of power available in the wind over a given time span, which is typically one year. For example, if the wind speed is 20 m/s, the available power is very large at that moment. However, if that speed is sustained for only ten hours per year and also if the wind speed is near zero the rest of the time, the resource for the year will be small. As a result, the wind speed distribution, which provides data on the frequency of occurrence of each wind speed, is critical in determining the resource at the location. This distribution is determined experimentally as the relative frequency of occurrence of uniform width wind speed ranges extending over the entire range of possible wind speeds (i.e., 0.5 m/s increments from 0 to 30 m/s).

This distribution may be approximated by a continuous curve, the probability density function, which corresponds to wind speed ranges of infinitesimal width. If the actual wind speed probability density distribution is not available, it is commonly approximated with the generalized two-parameter Weibull distribution given by:

$$f(\bar{u}) = \frac{k}{C}\left(\frac{\bar{u}}{C}\right)^{k-1}\exp\left(\frac{\bar{u}}{C}\right)^{k} \tag{2.1}$$

Where f($\bar{u}$) is the frequency of occurrence of wind speed $\bar{u}$, k is the Weibull shape factor and C is the Weibull scale factor.[62] It has been reported that Weibull distribution can give good fits to observed wind speed data. As an example, the Weibull distributions for various mean wind speeds are displayed in fig 2.4. The shape factor influences the coverage of wind speeds by the probability curve whereas the scale factor indicates the wind speed with higher probability of occurance.
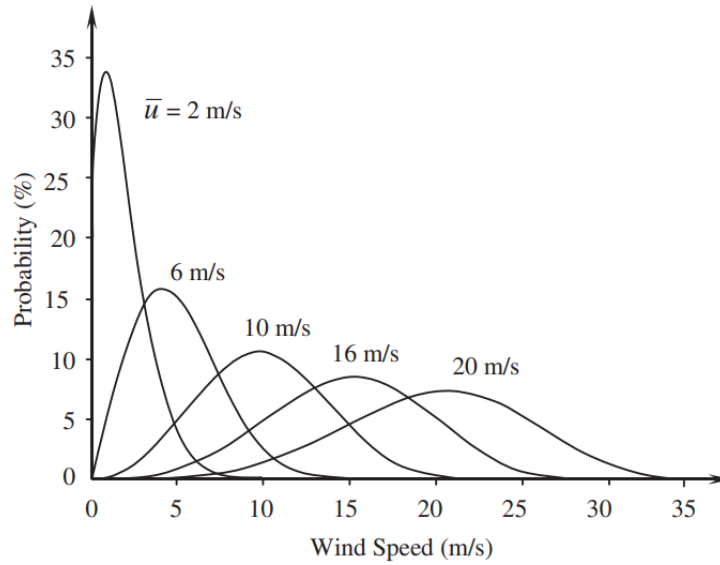
Figure 2.4: Weibull distributions for various mean wind speeds.[55]

Wind shear is a meteorological phenomenon in which wind increases with the height above the ground. The effect of height on the wind speed is mainly due to the roughness on the earth's surface and can be estimated using the Hellmann power equation that relates wind speeds at two different heights:

$$u(z) = u(z_0) \left(\frac{z}{z_0} \right)^{\alpha} \tag{2.2}$$

Where z is the height above the earth's surface, z_0 is the reference height for which wind speed $u(z_0)$ is known, and α is the wind shear coefficient. In practice, α depends on a number of factors, including the roughness of the surrounding landscape, height, time of day, season, and locations. Wind shear coefficients are typically lower during the day and higher at night. Wind shear often follows the "1/7 power law" meaning that α usually is equal to 1/7, according to empirical results.[55]

The significance of characterizing wind speed variation with elevation, or wind shear, at a particular site for a utility-scale wind turbine cannot be overstated since such characterization is required for more accurate power production prediction. Thus, the wind speed characteristics at turbine hub height and across the rotor must be precisely known.[36]

2.1.6 Wind Power Conversion

A wind turbine turns wind energy into electricity using the aerodynamic force from the rotor blades. The presence of the turbine causes the approaching air, upstream, gradually to slow down such that when the air arrives at the rotor disc its velocity is already lower than the free-stream wind speed. The stream-tube expands as a result of the slowing down and, because no work has yet been done on, or by the air, its static pressure rises to compensate for the decrease in kinetic

energy. When passing through the rotor, there is a sudden drop in flow pressure, in such a way that its value at the exit is lower than the pressure in the surrounding environment. Downstream of the rotor the pressure gradually increases until it reaches the atmospheric pressure value again, and velocity decreases according to a conversion process. This phenomena allows the rotor to spin as the lift force is greater than the drag. Between two distant points, one upstream and the other far away downstream of the rotor, the static pressure values are the same, but there is a deficit in kinetic energy, that is converted into mechanical energy by the rotor blades.

The conversion of wind energy to electrical energy involves primarily two stages: in the first stage, kinetic energy in wind is converted into mechanical energy to drive the shaft and then, with the aid of a wind generator, this energy is converted to electrical power and then conducted to the electrical grid with the aid of a proper controller to avoid the disturbances and to protect the system.

As stated before, the speed of the wind approaching a wind turbine is significantly reduced after it passes through it. Therefore there are two types of wind speeds that are referred as the higher speed before reaching the wind turbine and lower speed after it passes through the wind turbine. Thus, by resorting to the reduced wind speed, after it passes through the turbine, it is possible to calculate the amount of extracted power.[30] For that purpose, firstly, the kinetic energy of the wind is calculated resorting to the expression:

$$U = \frac{1}{2}mv^2 \qquad (2.3)$$

Where m is the parcel mass in kg and v is the wind velocity in m/s^2. When wind passes through a wind turbine and drives blades to rotate, the corresponding wind mass flow-rate is:

$$\dot{m} = \rho A v \qquad (2.4)$$

Where ρ is the air density in kg/m^3 and it is a function of altitude, temperature, and humidity, and A is the swept area of blades in m^2. At sea level and at 15 °C, air has a typical density of 1.225 kg/m^3 [60], and its the mos common value used for calculation of normal wind power production. From the expression 2.5, it is possible to obtain the kinetic power present in the wind by substituting equation 2.4 in the resulting time differentiated 2.3 expression, where r is the blade radius given in meters, resulting in:

$$P_w = \frac{1}{2}\rho A v^3 \quad ,\text{where} \quad A = \pi r^2 \qquad (2.5)$$

However, all the available energy in the wind cannot be harvested as stated by the german scientist Albert Betz who showed that an ideal loss-less wind turbine can only convert 59.3% of the total wind energy.[30] Thus, mechanical power P_t extracted from the wind kinetic power P_w is given by the following equation:

$$P_t = P_w \times C_p \qquad (2.6)$$

Where C_p represents the power coefficient of rotor blades and defines the portion of the power that is extracted from the wind. The power coefficient, therefore, depends on the aerodynamic design of the wind turbine. In order to obtain the turbine power coefficient, different measurements at various wind velocities were taken and the turbine power coefficient was estimated from an post process analysis. Analytical methods may also be applied in order to study the turbine's power coefficient. Manufacturers provide the turbine's power coefficients curve that correlates the power output variation with the power coefficients at different velocities.[30] For the new generation of high-power wind turbines, the C_p value ranges between 0.32 and 0.52.[60] Manufacturers also usually give information about the power curve of the wind turbines produced by them that is composed by the power output of that turbine for a range of speeds.

The power output of mechanical energy captured by wind turbine blades can also be given by:

$$P_t = \frac{1}{2}\rho A \bar{u}_2(\bar{u}_1{}^2 - \bar{u}_3{}^2) = \frac{1}{2}\rho A \bar{u}_1{}^3 4a(1-a) \tag{2.7}$$

Where $\bar{u}_1$ and $\bar{u}_3$ represent the mean velocities far upstream and downstream from the wind turbine, $\bar{u}_2$ is the mean velocity just in front of the wind rotating blades and a is the axial induction factor, defined as:

$$a = \frac{\bar{u}_1 - \bar{u}_2}{\bar{u}_1} \tag{2.8}$$

Substituting equation 2.8 into 2.6, yields:

$$C_p = 4a(1-a)^2 \tag{2.9}$$

This indicates that the power coefficient is only a function of the axial induction factor a. By deriving the expression above it was found that the maximum power coefficient reaches its maximum value of 16/27, when $a = 1/3$.[55]

The disparity between the P_t and the mechanical input power, P_m, values is represented by losses in the mechanical parts.[60] This losses are mainly due to the gearbox's power losses that can be divided into load-dependent and no-load power losses. Gear tooth friction and bearing losses are among the load-dependent losses, and oil churning, windage, and shaft seal losses represents the no-load losses. Thus, there is an efficiency associated to this process, η_{gear}.[55]

The wind generator then transforms the P_m into electric power, P_s. As the the generator's output voltage and frequency varies according to the wind speed, the generator's output power P_s is regarded as being unregulated. In order to stabilize these two parameters, a power converter is used, which regulates the electric power, while complying with the grid code requirements. Hence, the regulated electric power P_g is fed to the utility grid. In order to connect the wind turbines to the utility transmission network, a step-up transformer is usually used to boost the output voltage of the power converter.[60]

All electrical and mechanical losses in the wind generator, such as copper, iron, load, windage, friction, and other miscellaneous losses are related to the generator efficiency, η_{gen}. However, on

the other hand, the electric efficiency, η_{ele}, is responsible for measuring the amount of power that remained after all combined electric power losses in the converter, switches, controls, and cables.[55] Therefore, the total power conversion efficiency from wind to electricity η_t is the product of these parameters, as in the following equation:

$$\eta_t = C_p \eta_{gear} \eta_{gen} \eta_{ele} \tag{2.10}$$

Thus, by identifying all the values that correspond to variables above mentioned, it is possible to calculate the final effective power that is fed to the utility grid.

$$P_g = \eta_t P_t = C_p \eta_{gear} \eta_{gen} \eta_{ele} P_t \tag{2.11}$$

Resorting to figure 2.5, a block diagram is presented containing all the variables cited before for a better comprehension of the energy conversion process and its corresponding losses.
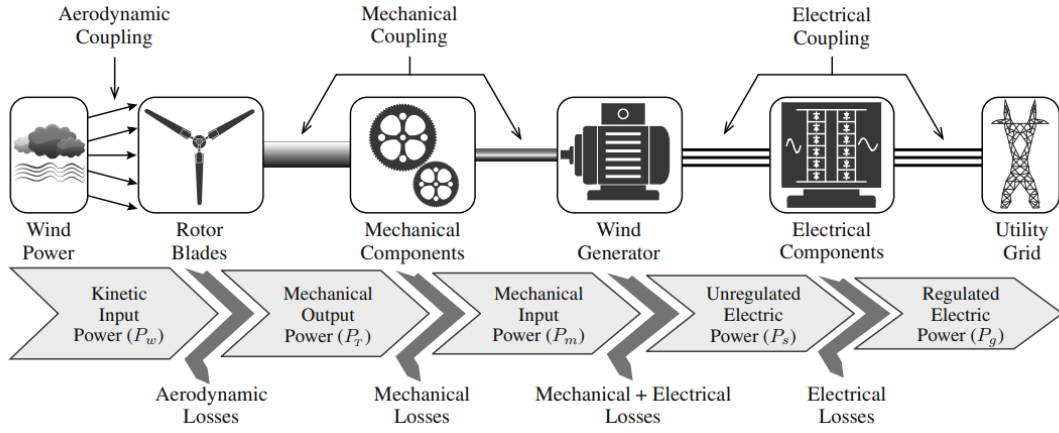
Figure 2.5: Block diagram of wind kinetic energy to electric energy conversion system.[60]

Ultimately, it is important to refer that, for a wind turbine to work, the wind speed should be higher than the cut-in speed that is the lowest wind speed after which the turbine starts to produce usable power. WTs also present a cut-out speed that is the limit speed upon which the nominal power or the maximum power that the turbine can generate is achieved. If the wind speed surpasses in a great amount the cut-out speed, the controller can command the turbine to stop stopping the power generation, in order to reduce the fatigue and stress associated to the operation of the wind turbine at that high wind speeds. Nonetheless, the energy output of the wind turbine is calculated using equation 4.3.

$$P_{WT} = \int_0^\infty f(v) P_c(v) dv \tag{2.12}$$

Where f(v) is the probability distribution function, $P_c(v)$ is the wind turbine power output function and P_{WT} is the average hourly power production of the wind turbine. Therefore the

annual power output, E_{WT}, can be calculated by multiplying the average power generation by the number of hours within a year, following 4.3:

$$P_{annual} = P_{WT} \cdot 8760h \tag{2.13}$$

2.2 Hydrogen

As a flexible energy source for the manufacturing and transportation industries, hydrogen is a suitable component for the power grid of the future. Since refinery consumption is expected to decline, the European Green Pact (EGP) forecasts an increase in the demand for renewable hydrogen. However, the demand for hydrogen production will increase as a result of the widespread decarbonization of the chemical and metallurgical sectors. Capital development options to address the increase in energy demand include granting a secure and reliable power grid operation that supports this energy transition.[18] However, according to the EU's hydrogen strategy, at least 6 GW of electrolysers powered by renewable energies are projected to be installed between 2020 and 2024 and the total amount of electrolysers could increase to 40 GW by 2030. Depending on its utilization, such capacity could produce up to 0.8 Mt of clean hydrogen, annually. Renewable hydrogen or green hydrogen, which costed five euros per kilogram in 2020, is essential for reaching zero net greenhouse gas emissions from electrolysis and using renewable sources as fuel. Hydrogen production using wind energy is anticipated to cost around two euros per kilogram by 2030. Electrolyser's costs are projected to halve by 2050, while renewable electricity costs will continue its tendency to continuously lower the price.[29]

2.2.1 Hydrogen Production

Upon transmitting the electricity generated by the wind turbines from the wind farm to the hydrogen production facility, the power undergoes a crucial process. This process involves passing the connection through electrical power stabilizers to maintain a consistent voltage flow. Subsequently, the stabilized output voltage is channeled through rectifiers, which convert it into a suitable direct current output. This DC output is essential to ensure the efficient and smooth operation of the electrolyser. Afterwards, in order to produce hydrogen, it is necessary that the electricity passes through two electrodes.[46] The hydrogen produced can be storage into high pressure tanks or it can be fed directly to a pipeline. The hydrogen production process is shown in the flow chart in figure 2.6.

2.2.2 Water Electrolysis

Demineralized water can be decomposed using direct electric current, and hydrogen and oxygen will be produced from the water through redox reactions. The overall reaction is represented by:
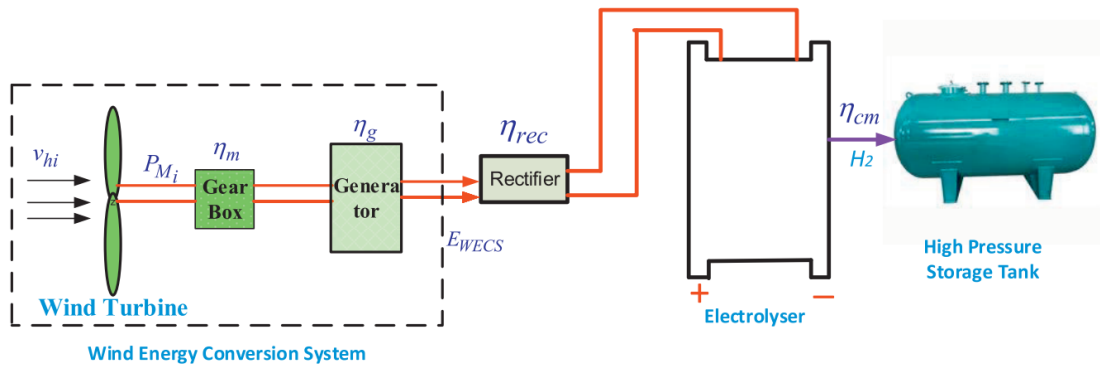
$$H_2O \rightarrow H_2 + \frac{1}{2}O_2 \tag{2.14}$$

Figure 2.6: Block diagram of the wind kinetic energy to hydrogen conversion system.[46]

The mechanism that combines the oxidation and reduction processes to generate hydrogen and oxygen gas is known as an electrolyser. In theory, an electrolyser can be connected to any electric power generation source, such as a fossil fuel, biomass electric power facility, nuclear power, solar, wind and other renewable energy sources. However, in this study all emphasis will be given to the production of hydrogen from a wind energy power source.[65] While different technologies for electrolysers operate in slightly different ways, all have an anode and cathode that are separated by an electrolyte in the middle.[23]

For this process. the electrodes must possess necessary structural qualities, high catalytic activity, powerful electric permeability, and a resistance to corrosion. Any change in the electrolyte during the process must be prevented, since the electrolyte must not interact with the electrodes. During the electrolysis procedure, a diaphragm or separator is required to stop the hydrogen and oxygen generated at the electrodes from recombining. The conductors are shielded from short-circuiting by the electrical resistance of the diaphragm. Additionally, the diaphragm needs to have a high ionic permeability so the hydrogen and oxygen ions can pass through it and must also possess high levels of chemical and physical stability. The electrolytic cell is composed by an assembly of conductors with the diaphragm, and the electrolyte.[64]

Three different types of electrolyte can be used in a typical electrolysis process, namely, a liquid electrolyte, a solid polymer electrolyte in the form of proton conducting membrane, or oxygen ion conduction membrane. Thus, according to the adopted electrolyte type, there are three types of electrolysers, the alkaline electrolyser, the proton exchange membrane or the polymer electrolyte membrane electrolyser (PEMEL) and the solid oxide electrolyser (SOE).

2.2.2.1 Alkaline Electrolysers

Alkaline electrolysers (AELs) are currently the cheapest technology and have the longest lifetime, due in part to being the oldest of the technologies mentioned above since this type of electrolyser has been used in the industry for roughly 100 years. Thus, further progress is expected, however the development of both PEMEL and SOE will surely be faster.[23]

AELs is considered safe and efficient, and it has relatively inexpensive investment costs compared to other technologies since it does not employ precious and expensive materials such as the PEMEL, for example. A common AEL runs between 60 and 80 °C with a current density of roughly 400 mA/cm^2 and cell voltages values between 1.85 and 2.2 V.[57]

AELs comprises two electrodes, a cathode and an anode, kept apart by the diaphragm, all submerged in a liquid electrolyte solution to promote the reaction. The application of an electrical direct current leads the electrodes to create oxygen and hydrogen at the anode and the cathode, respectively. The diaphragm permits the passage of ions while preventing the generated gases from passing through to avoid their mixing.[64] The following reaction is expressed in reactions 2.15 and 2.16:

Anode:

$$2OH^- \rightarrow \frac{1}{2}O_2 + H_2O + 2e^- \tag{2.15}$$

Cathode:

$$2H_2O + 2e^- \rightarrow H_2 + 2OH^- \tag{2.16}$$

The most common electrolyte is a 30% concentrated liquid of potassium hydroxide (KOH), however sodium hydroxide and sodium chloride can also be used for this purpose. The diaphragm can be made of ceramic oxides such as asbestos and potassium titanate, or also polymers such as polypropylene and polyphenylene sulfide.[57] The most commonly material that was used to produce the diaphragm, in conventional AELs, was a three millimeter thick asbestos, a naturally occurring mineral. Nevertheless, it is gradually being replaced with alternatives due to health risks and because it prevents the AELs operating temperature from exceeding 80 °C due to its heat resistance properties. The anode is made of steel with a nickel coating, and the cathode is made of steel with a catalyst coating.[64] Today, the major electrolyser producers such as *Nel Hydrogen (Norway), Hydrogenics (Canada), Teledyne Energy Systems (USA)* and *De Nora (Italy)* are using non-asbestos separators, with the chemical composition of their separators remaining a hidden secret as it remains their competitive advantage.[26]

However, they cannot react as fast to changes in production as other technologies, require complex maintenance of the fluid and cannot operate below a certain threshold for safety reasons. In addition, the output pressure of the hydrogen produced is lower, which requires higher compression for transport and storage, reducing the advantage given by the lower CAPEX[1] stated initially.[23] In the past years, research had been focused on reducing the operating costs associated to the consumption of electricity hence improving the efficiency. Meanwhile, the operating current densities have been increased in order to reduce the investment costs.[65]

New pressurized AELs systems have recently been created. These systems can, in a more effective way, adjust to changes in power input, which makes them ideal for use in combination

---

[1]CAPEX, refers to funds that a company invests in long-term assets to increase capacity, improve quality, or reduce operating costs.

with renewable energy sources and enables them to compete with other technologies like PEM electrolysis. Another advantage of pressured electrolysis is that it requires less energy to compress hydrogen to storage pressure levels. However, due to the diaphragm's increased permeability at high pressures and temperatures, it can also result into a decline in the quality of the gases produced, which has a detrimental effect on the efficiency of the entire process.[20]

A study conducted by the Yodwong et al.[61], concluded that among all leading alkaline electrolyser in the market, the Norwegian company *NEL* proposes the best alkaline electrolyser in terms of operating pressure, hydrogen flow rate, specific energy consumption, partial load range, and stack power. The A-series can use two 2.2 mW stacks connected in series to boost power and hydrogen flow rate while lowering specific energy consumption and providing a wide partial load range.
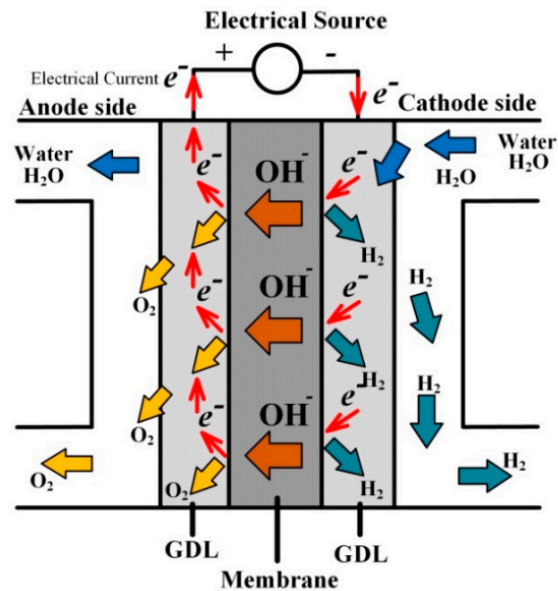
Figure 2.7: Alkaline Electrolyser.[61]

2.2.2.2 Polymer Exchange Membrane Electrolyser

A thin, solid polymeric membrane with a thickness of less than 0.2 mm and an acidic character serves as the electrolyte, revelling to be the major difference between PEMELs and AELs that use a corrosive liquid electrolyte instead.[65][56] It is composed by functional groups of the sulfonic acid class that carry protons through an ion exchange process. Some PEMEL designs may achieve pressures of up to 8.5 MPa, allowing the synthesis of oxygen at air pressure while producing hydrogen at 3.5 MPa and eliminating the risks of handling pressurized oxygen. PEMELs operate between 50 and 80 °C and their efficiency varies from 56% to 60%.[56]

For this process to occur, high purity deionized water is required for the electrolysis process. At the anode, water is oxidized to produce oxygen, electrons and protons. The protons will travel

across the proton exchange membrane to the cathode side while the electrons will reach the cathode side via an external circuit. At the cathode, protons will be reduced to generate hydrogen. The following reactions take place in a PEMEL[65]:

Anode:

$$H_2O \rightarrow \frac{1}{2}O_2 + 2H^+ + 2e^- \quad (2.17)$$

Cathode:

$$2H^+ + 2e^- \rightarrow H_2 \quad (2.18)$$

PEMELs, which are more modern than AELs, provide a number of benefits, including a much faster start-up times, higher current densities that result in smaller electrolyzer footprints, higher hydrogen purity (>99.8%) and operation beyond nominal power.[23] Furthermore, it can also produce highly pressurized hydrogen for decentralized production and storage at refueling stations and are comparatively small, enabling its possible use in populated areas.[56] The PEMEL is more suitable to work under fluctuating power supply due to the fact that the transportation of protons across the membrane that has a quick response to fluctuating power supplies.[65]

Despite recent improvements in efficiency, output pressure and CAPEX, PEMELs are still significantly more expensive than AELs and do not have the same lifetime. The huge amount of platinum required to construct the electrolyzer's stack result in higher manufacturing cost and its the primary reason for the elevated price.[23] However, by analysing each factor mentioned above it is possible to concluded that the PEMEls can be more applicable commercially than the alkaline water electrolysers depending on the type of use required.[26]
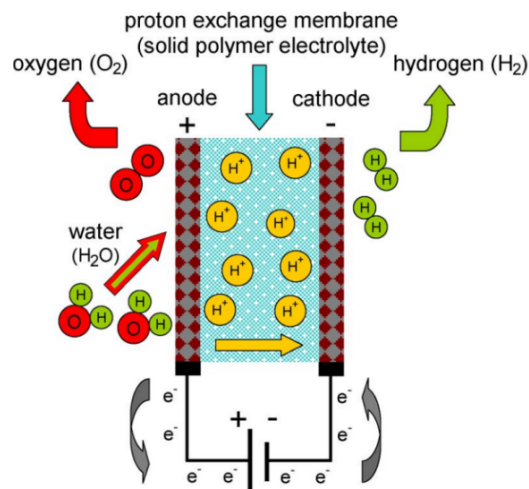
Figure 2.8: PEM Electrolyzer.[56]

2.2.2.3 Solid Oxide Electrolysers

Due to its high operating temperatures, typically in the range of 700-900 °C, and lower longevity[23], the SOEs are the newest of the previous mentioned technologies, that usually operate at low temperatures, about 100 °C,[65] however nowadays these are rarely used in commercial applications. This type of electrolyser promises greater efficiency compared to all other technologies and, unlike PEMEL, does not require the use of precious metals.[56]

SOE was created with the aim of lowering energy demand and, as a result, operational costs. SOE is made of Yttria-stabilized zirconia (YSZ), which benefits from oxygen vacancies in the mixed oxide structure to provide excellent ionic conductivity even at high operating temperatures. The anode is made of YSZ and perovskites, a rare mineral, which are designed to promote electro-catalysis reactions through structural and electronic flaws, whereas the cathode is made of nickel and YSZ.[56]
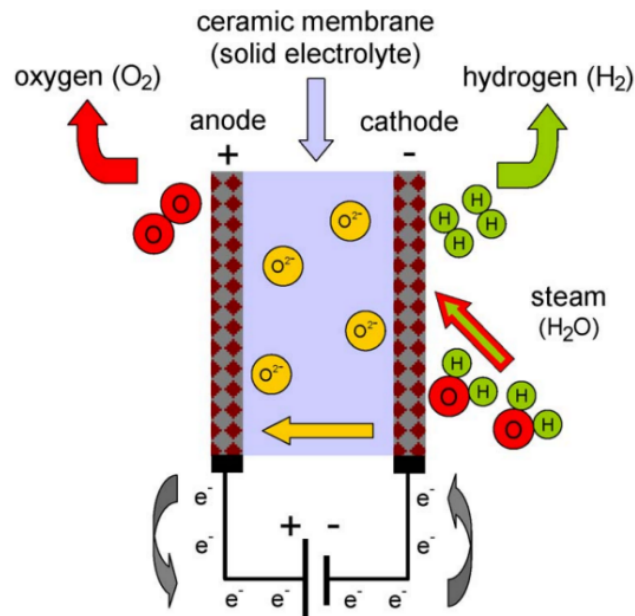
Figure 2.9: SOE Electrolyser.[56]

This technology utilize steam rather than liquid water and as mentioned before, this type of electrolyser requires a high temperature heat supply, that can be obtained from energy sources such as nuclear reactors, geothermal energy or solar thermal energy, since, the higher the temperature is, the less electrical energy is needed for the electrolysis. Theoretically, SOEs with steam electrolysis at 1000°C can cut the requirement for electricity by up to 25% when compared with other electrolysers.[10][56]

Even though SOE is available commercially, AEL and PEMEL are more developed and frequently utilized. With SOE, research efforts are focused on commercialization, increasing output,

prolonging the life of products, and reducing costs.[5] SOEs suffer from degradation due to mechanical stress resulting from the high operating temperatures and also have greater capital costs due to the necessity for additional processing of the hydrogen-steam mix generated at the cathode.[56] SOE still needs to advance in those aforementioned areas in order to compete with the other conventional methods.[5] Once it matures, it will become possible this technology to achieve a lower CAPEX.[23]

SOE is not suitable for fluctuating power input since the interminent changes in load that cause heat losses and changes in the cell's temperature, that ultimatly lead to micro cracks in the membrane, reducing significantly the electrolyser's lifespan .[65] For all the aforementioned reasons SOEs are not commonly used in hydrogen production from wind energy. However, the mention of this technology was seen as necessary since its development is increasing and its the most recent currently used state-of-the-art electrolyser technology.

The mature technologies available for producing hydrogen through water electrolysis are alkaline and PEM technologies discussed above. However, more technologies in this area are sprouting and are currently in the research and development stage. Table 2.2 shows a comparison, in various parameters, of this three different water electrolysis methods.

Technology	Alkaline electrolyser	PEM electrolyser	Solid oxide electrolyser
Technology status	Mature technology	Mature technology	Lab-scale, R&D
T range (°C)	Ambient / 120	Ambient / 90	800 / 1 000
Electrolyte /pH	25-30 wt% (KOH)	PFSA[1]	Zirconium dioxide (ZrO_2) derivates
Mobile species	OH^-	H_3O^+	O^{2-}
Cathode catalyst	Nickel foam/Ni-SS[2]	Platinum	Ni-YSZ or Ni-GDC Cermet
Anode catalyst	Ni_2CoO_4, La-Sr-Co_3O_3, Co_3O_4	Ir/Ru oxide	(La, Sr)MnO_3, (La, Sr)(Co_3Fe)O_3
Separator	Asbestos	Electrolyte membrane	Electrolyte membrane
Current distributor	Nickel	Titanium	Ferritic Stainless Steel
Sealent	Metallic	Syntethic rubber of fluoroelatomer	Glass and vitro-ceramics
Containment material	Nickel plated steel	Stainless Steel	Stainless Steel
Water specification	Liquid	Liquid	Steam
Conventional current density (A/cm²)	0.2-0.5	0-0.3	0-2
Max. nominal power per stack (MW)	6	2	<0.01
H_2 production per stack (Nm^3/h)	1400	400	<10
Efficiency (%, LHV)	63-70	56-60	74-81
Stack lifetime (operating hours$*10^3$)	60-90	30-90	10-30
Load range (% relative to nominal load)	15-100	0-100	20-100
Investment costs (€/kW)	800–1500	1400–2100	(> 2000)

Table 2.2: Comparison of different types of electrolysers.[56] [37] [22] [1] PFSA: perfluorosulfonic acid. [2] Ni-SS: nickel-stainless steel.

2.3 Hydrogen Storage and Distribution

The intermittent nature of renewable energy resources, such as wind and solar, can make the delivery of energy less predictable, which may result in mismatches in the power network. To that end, hydrogen production and storage can provide an answer by increasing the system flexibility. Thus, hydrogen stored as compressed gas can be converted back into electricity or used as a feedstock for many applications, such as heating, it as various uses at an industrial level and can also be used as a car fuel.

Hydrogen storage plays a pivotal role in advancing the hydrogen economy. Its applications vary, and the development of storage methods is both challenging and crucial. In the transportation sector, there is a preference for storing H_2 in lightweight and secure containers with high density, as weight significantly affects efficiency. Conversely, in stationary applications, a higher volumetric density is favored, as weight is not the primary factor influencing system efficiency.[65]

Hydrogen can also be injected directly into existing natural gas pipelines, creating a blend of hydrogen and natural gas. This blend can then be transported through the existing pipeline infrastructure to various locations, where it can be used as a source of clean energy, representing a promising solution to enhance the competitiveness of wind farms, contributing to a more economically viable and sustainable energy market.

2.4 Fuel Cell

Fuel cells is responsible for directly converting the chemical energy in hydrogen to electricity, with pure water and potentially useful heat being the only byproducts. In this system, hydrogen and oxygen interact through the following electrochemical reaction[17]:

$$H_2 + \frac{1}{2}O_2 \rightarrow H_20 + \dot{W} + \dot{Q} \tag{2.19}$$

Where $\dot{W}$ represents the heat rate is produced and $\dot{Q}$ is the electric power output. Hydrogen and oxygen (O_2) are chosen as the fuel and oxidant, respectively, in fuel cell systems. This technology represent a modern energy conversion tool capable of producing electric power in a single step without any moving parts. Unlike conventional combustion-based power plants that typically achieve electricity generation efficiencies of 33 to 35%, fuel cell systems can achieve efficiencies of up to 60%, which can be further increased with cogeneration. This represents an efficiency twice as high as traditional combustion technologies.[17][44]

A single fuel cell consists of an electrolyte that is placed between an anode and a cathode, that are designated as electrodes, similar to the configuration within an electrolyser. The anode of a fuel cell receives a supply of hydrogen gas, which undergoes a reaction that results in the separation of hydrogen molecules into protons and electrons caused by a catalyst. The electrons are directed through an external circuit to the cathode, in order to generate usable electricity, as the membrane selectively permits the passage of only the protons.[58]

The cathode of the fuel cell possesses channels to allow the flow of air. Once the electrons return from powering a specific external circuit, they combine with oxygen from the air and with the protons that have crossed the membrane. Together, these components undergo an exothermic reaction, resulting in the formation of water. This reaction releases heat, which can be effectively used for external applications such as heating instead of being lost to atmosphere. Figure 2.10 allows a more visual representation of the process described above.
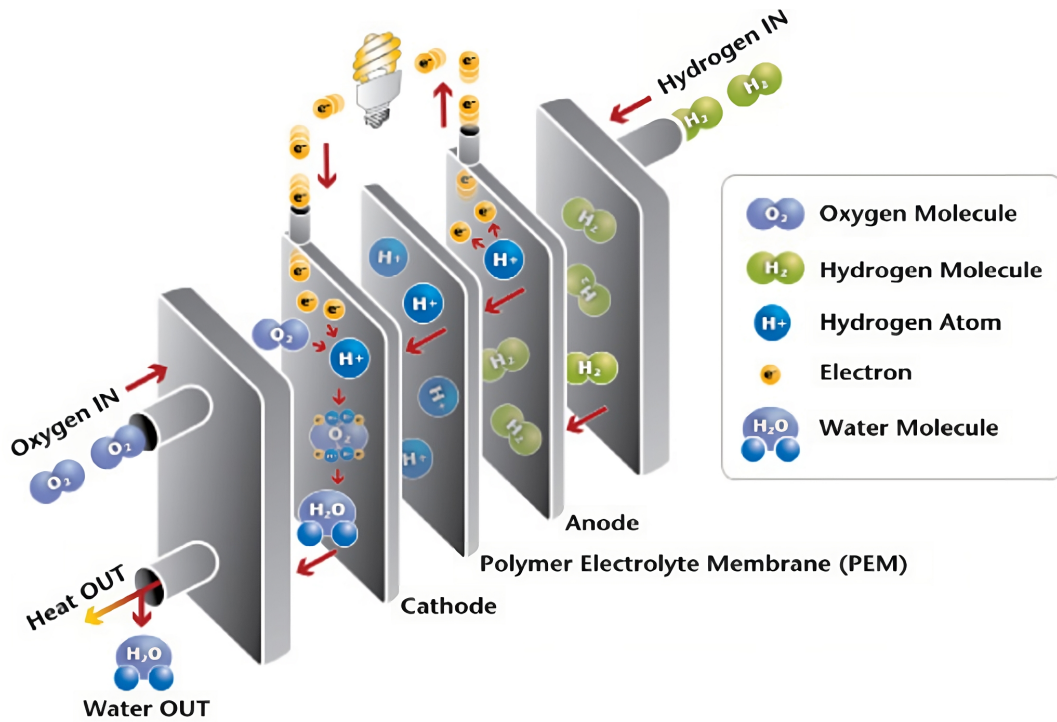
Figure 2.10: PEM fuel cell.[44]

To enhance the voltage output, multiple fuel cells are interconnected in a series arrangement, forming, what is commonly referred to, as a stack. The composition of a fuel cell stack can vary depending on the specific requirements of the application and the output power needed, encompassing a range that can go from a few cells to hundreds of cells stacked together.[44]

Although fuel cells share a fundamental configuration, they can be categorized into different types, based on the specific electrolyte employed. These classifications are primarily determined by the type of electrolyte used and are outlined in table 2.3.

Nevertheless, there is a significant energy loss during the conversion process from energy to hydrogen and back and as a result, the overall efficiency of the process is currently not that high. Additionally, at this early stage, the implementation cost of fuel cell technology remains high, thus one of the future goals is to surpass the performance of traditional power technologies by also improving its efficiency and its lifespan. With this aim in mind, continuous efforts are focused on identifying and developing new materials that can reduce costs and prolong the lifespan of fuel cell stack components. Furthermore, the adoption of low-cost, high-volume manufacturing processes

will contribute to make fuel cell systems more cost-competitive when compared with traditional technologies.

Fuel Cell Type	Common Electrolyte	Operating Temperature	Typical Stack Size (kW)	Electrical Efficiency (LHV)
Polymer Electrolyte Membrane (PEM)	Perfluoro sulfonic acid	$< 120°C$	$< 1 - 100$	60%
Alkaline Fuel Cell (AFC)	Aqueous potassium hydroxide soaked in a porous matrix, or alkaline polymer membrane	$< 100°C$	$1 - 100$	60%
Phosphoric Acid Fuel Cell (PAFC)	Phosphoric acid soaked in a porous matrix or imbibed in a polymer membrane	$150 - 200°C$	$5 - 400$	40%
Molten Carbonate Fuel Cell (MCFC)	Molten lithium, sodium, and/or potassium carbonates soaked in a porous matrix	$600 - 700°C$	$300 - 3000$	50%
Solid Oxide Fuel Cell (SOFC)	Yttria stabilized zirconia	$500 - 1000°C$	$1 - 2000$	60%

Table 2.3: Comparison of fuel cell technologies.[44][59]

Power systems, that can be powered by fuel cells, operate at different ranges of input power. In the power range of 1–10 kW, fuel cells could be used to power mobile phones, laptops, personal digital assistants (PDAs), portable electronic devices, and similar applications. In the power range of 1–100 kW, fuel cells are suitable for powering automobiles and public transportation vehicles such as buses, cars, and mini-trains. Moreover, in the power range of 1–1 MW, fuel cells can be used for energy power systems that provide electricity and cogeneration systems.[17]

Each fuel cell technology presents unique advantages and challenges that must be considered for specific applications and system requirements. The following specifications outline some of the key characteristics of the fuel cell technologies currently available:[44][2][59]

- **Polymer Electrolyte Membrane (PEM):** One of the key advantages of PEM fuel cells is

their quick startup time, allowing for rapid power generation. Additionally, they exhibit temperature resistance, enabling operation in varying environmental conditions. The use of a solid electrolyte in PEM fuel cells helps mitigate corrosion and electrolyte management issues. Furthermore, these fuel cells are well-suited for low-temperature applications and can quickly adapt to varying power demands.

Despite their advantages, PEM fuel cells also present certain challenges. The inclusion of liquid catalysts adds weight to the system, that as a direct impact in portability and on its efficiency. Moreover, PEM fuel cells typically require larger sizes to accommodate their components and rely on expensive catalysts, making them costlier to manufacture and maintain. Furthermore, PEM fuel cells can be sensitive to fuel impurities, necessitating proper fuel purification and filtration systems, also increasing its maintenance cost.

- **Alkaline (AFC):** Alkaline fuel cells also offer quick startup times, making them suitable for applications requiring immediate power supply. These fuel cells are known for their compact and lightweight design, enabling their use in space-constrained systems with also exhibiting good performance at low temperatures. Furthermore, the wider range of stable materials, available for alkaline fuel cells, allows for the use of lower-cost components.

  However, AFCs also have their downside. They can be sensitive to humidity or dryness, requiring careful control of the operating conditions. Additionally, alkaline fuel cells may exhibit sensitivity to salinity and low temperatures, which must be addressed to ensure optimal performance. Proper electrolyte management is crucial in aqueous alkaline systems, and polymer-based AFCs since they require sufficient electrolyte conductivity for efficient operation.

- **Phosphoric Acid (PAFC):** Phosphoric acid fuel cells are known for their stability and maturity in the field of fuel cell technologies. They are particularly suitable for combined heat and power (CHP) applications, where they can efficiently re-utilize heat liberated, for example, from other power production technologies. PAFCs exhibit increased tolerance to fuel impurities, allowing the use of a wider range of feedstocks.

  While PAFCs offer advantages in specific applications, they also have limitations. Long startup times are a characteristic challenge associated with phosphoric acid fuel cells since the process of vaporizing phosphoric acid can take time, leading to delays in power generation. Additionally, PAFCs may have lower power densities compared to some other fuel cell technologies.

- **Molten Carbonate (MCFC):** Molten carbonate fuel cells provide advantages such as the ability to utilize a variety of fuel sources, enabling the use of different types of gases or liquid hydrocarbons, and high overall efficiency. MCFCs are well-suited for CHP applications, and they can be integrated into hybrid systems such as gas turbine cycles.

However, they can exhibit slow response times, requiring adjustments to maintain optimal performance. Moreover, the corrosive nature of the molten carbonate electrolyte necessitates careful selection of materials to ensure long-term durability.

- **Solid Oxide (SOFC):** Solid oxide fuel cells offer advantages such as high efficiency and fuel flexibility since they can operate on a variety of fuels, including hydrogen, natural gas, and biofuels. SOFCs feature a solid electrolyte, enabling stable and efficient operation. Similar to other fuel cell technologies, they can be integrated into CHP systems and hybrid configurations, such as gas turbine cycles.

Over the past few years, both PAFC and MCFC technologies have shown significant growth rates. However, it's important to note that this trend may change as an increasing number of companies are now offering PEMFC systems with capacities greater than 1 MW, and some of these systems are stackable modules. This evolving landscape suggests a potential shift in the market dynamics for fuel cell technologies. [59]

Chapter 3

Methodology

The following chapter focuses on the methodology used to develop the electrolysis-based hydrogen production model from wind energy along with the study of the functioning of the fuel cell. Firstly, all the relevant parameters to this end are defined, and afterwards, the mathematics models are introduced for every component present on the system. Subsequently, the input data is identified, and an appropriate database structure is created. Furthermore, the code program is written, and the desired output data and calculation scenarios are defined.

The model has been crafted to encompass all the essential considerations and approaches required for its application in the analysis and design of real-scale Wind-H_2 systems. Its implementation has been executed using Python, providing the flexibility for validation and execution of the model. This mathematical framework not only affords a understanding of the system's behavior but also streamlines its utilization for various design and analysis objectives.

3.1 Mathematical Modeling

3.1.1 Wind Farm

The entire process, from the origin of the collected wind speed data to the eventual power output, will be described. This will encompass all the requisite components in this calculation, complete with their respective formulas, to provide a detailed understanding of the process.

Wind velocity changes according to geographical location, time of day, season, height above the earth's surface, weather, and local orography. Understanding wind characteristics will aid in the optimization of the wind turbine design, the development of wind measuring methods, and the selection of wind farm sites. Wind speed is a useful parameter for evaluating a region's potential for producing wind energy. For the purpose of this work, velocity data was selected and obtain resorting to the *POWER Data Access Viewer* platform that was developed by *NASA*. The *POWER Data Access Viewer* contains geospatially enabled meteorology related parameters formulated for assessing and designing renewable energy systems.[52] This meteorological parameters are derived from the *NASA's Global Modeling and Assimilation Office MERRA-2* assimilation model. *Modern-Era Retrospective analysis for Research and Applications*, Version 2 (*MERRA-2*) is the

first long-term global reanalysis to assimilate space-based observations of aerosols and represent their interactions with other physical processes in the climate system.[6] This platform allows to retrieve information about wind speed and direction in any desired place with known coordinates regarding latitude and longitude. The time interval in which this data is comprehended can be selected in the *POWER Single Point* mainframe and its variation can be hourly, monthly or annually. The wind data collected posses an hourly variation, within a year, in order to analyse in more detail the dissimilarity between wind speeds at a given hour and day, and consequently present a more accurate prediction.

Wind turbines generate power by harnessing the kinetic energy of the wind. The amount of energy that can be produce is determined by a variety of factors among which it is possible to highlight the wind speed, the size and design of the turbine blades, and the efficiency of the generator. An analysis of the mathematical formulas, that dictate the generation of power within a wind turbine or farm, allows to predict and understand the amount of energy that a system can produce. By implementing this framework, a wind turbine model can be developed with the aim of characterizing the real behaviour of a wind farm within a specific location. With the data collected using the platform mentioned in the aforementioned paragraph, a graphic visualization of the variation of the wind speed and its frequency can be employed to understand the profile of the wind speed at a given location. Furthermore, wind direction is a significant element in wind energy analysis and has a critical impact in identifying the optimum positioning for wind turbine installations. For this purpose, the frequency for which the wind direction falls within different sectors should be identified. It is indispensable to generate a wind rose in order to assess the predominant wind direction to align the wind turbines according to this direction. A wind rose contains a visual representation of the distribution of wind speed and direction at a specific area. The frequency of winds over a lengthy time period is plotted by wind direction using a polar coordinate system of gridding, with color bands denoting wind ranges. Each concentric circle represents a different frequency, emanating from zero at the center to increasing frequencies at the outer circles.[40]

The wind data obtained resorting to the *POWER* software is estimated at two different elevations from the ground, generally, 10 and 50 meters. In large scale grid power generation, such as a wind farms, the hub of the wind turbines is usually at a higher height than the ones where this wind measures were retrieved. As a consequence, the speed at the hub´s height should be calculated in order to reduce the errors associated with the prediction of the power production by the wind farm. Therefore, the relevance of characterizing wind speed variation with elevation, or wind shear, at a particular site cannot be overstated. Wind shear is the meteorological phenomenon in which wind increases with the height above the ground. The effect of height on the wind speed is mainly due to roughness on the earth's surface and can be estimated using the Hellmann's power equation that relates wind speeds at two different heights following equation 2.2:

Instead of assuming that wind shear coefficient is equal to 1/7, it is possible to calculate this coefficient for the wind profile in question. The accessed data includes records of wind speed at two distinct heights for a sufficient period of time.[19]:

$$\alpha = \frac{\ln(u(z)) - \ln(u(z_0))}{\ln(z) - \ln(z_0)} \qquad (3.1)$$

At the present case, the value of α is calculated by substituting the variables in equation 3.1 by the wind speed values at the height of 10 and 50 meters and their respective height. Since the wind speed values vary from hour to hour, the wind shear coefficient also exhibits an corresponding variation. Therefore, in order to adapt to the changing wind profile, the value of the wind shear coefficient used was calculated as the average of the wind shear, for each hour.

By resorting to the values computed for the wind shear coefficient, it becomes feasible to estimate the wind speed at the hub height of the turbine. This estimation can be achieved by substituting the variable z with the height of the turbine's hub in equation 2.2, considering that $u(z_0)$ and z_0 are already known parameters.

The following step would involve evaluating the most suitable wind turbine to install at the given location, aiming to maximize the power that can be extracted from the wind resource. This is a crucial step as it enables the maximization of the wind resource potential in the region. At this phase, the focus is primarily on technical considerations rather than economic factors. By comparing the outcomes of multiple wind turbines, it becomes possible to select the turbine with the highest efficiency, ensuring optimal utilization of the available wind resources.

By definition, a wind farm consists of multiple wind turbines strategically placed to harness the full extent of the region where it is located. This configuration allows for the exploitation of a larger area and maximizes power generation potential, particularly in regions characterized by strong winds. However, as the number of wind turbines installed in wind farms increases, the impact of the wake effect and the loads generated by it become more significant. The wake of a wind turbine occurs in the area downstream of the turbine, where the flow is affected by the wind turbine absorbing momentum from the incoming wind, resulting in a decrease in wind speed in the downwind region as represented in figure 3.1. However, the flow within the wake is more turbulent compared to the incoming wind flow. This turbulence is caused by the rotation of the wind turbine blades and the obstruction of the incoming flow by the wind turbine itself. In wind farms, downwind wind turbines experience increased structural loads and reduced wind speeds due to the wakes created by upstream wind turbines, that can generate wind gust as the wind can vary in an intermittent regime. This reduction in performance has a significant impact on the overall efficiency of the wind farm. Therefore, gaining a better understanding of wake characteristics is crucial to gain insights and implement measures to mitigate the wake effects on downstream wind turbines. [53]

The speed decay within the wind farm must be considered to ensure accurate power estimation. Using the same wind speed values for every turbine would lead to an overestimation of power. To mitigate this error, a model is employed to account for the speed reduction within the wind farm. The model employed was the Jensen wake model that assumes a linearly expanding wake, where the velocity deficit is solely determined by the distance behind the rotor. Jensen's model treats the wake as a turbulent flow and neglects the contribution of vortex shedding, which measures the
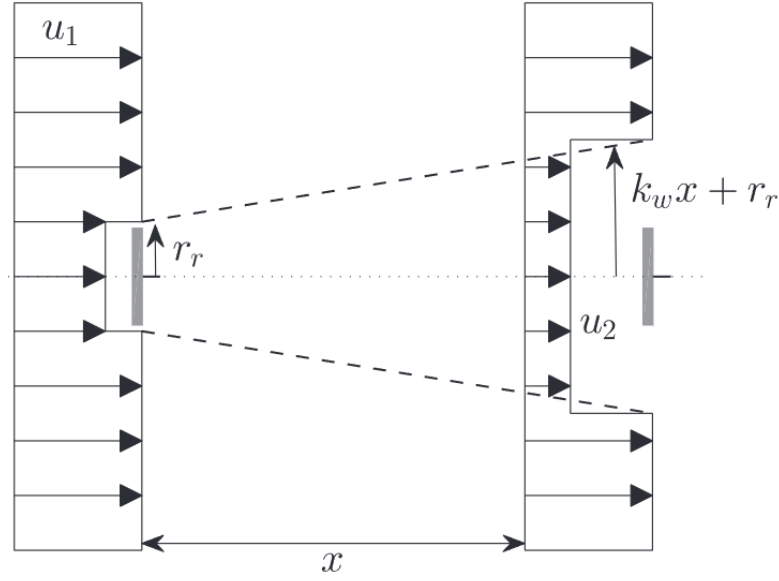
Figure 3.1: Jensen's single wake model.[45]

rate of wind rotation and is only significant in the near wake region. The derivation of this wake model is based on the conservation of momentum downstream of the wind turbine. The velocity in the wake is described as a function of the downstream distance from the turbine hub, and it is assumed that the wake expands linearly as it moves downstream.[49]

$$v_1 = v_0 \cdot \left(1 - \frac{1 - \sqrt{1 - C_t}}{(1 + 2\alpha s)^2}\right) \tag{3.2}$$

Equation 3.2 represents the wind velocity within the confined area of a single turbine's wake, which forms the fundamental approach of Jensen's single wake model, where C_t the thrust coefficient of upwind turbine and it is a function of the induction factor and is estimated to have the value of 0.075, s is equal to $D/2r$ where r is the rotor radius. D is the relative distance behind the rotor and, for the purpose of this study, it was assumed that the distance between each wind turbine is equivalent to four times the size of the diameter of the rotor. In most land cases, the default decay constant value for the wind speed is 0.075, while for offshore applications, it is recommended to use a decay constant value of 0.04.[53][49]

The severity of the wake effect intensifies as the number of wind turbines within a wind farm increases, as well as in the presence of neighboring wind farms. In this scenario, a single target turbine can be influenced by the wakes generated by multiple turbines, leading to what is known as the multiple wake effect. To account for the multiple wake effect, Jensen's multiple wake model is employed to calculate the wind speed. This model considers the interactions and impact of wakes generated by multiple turbines on the wind speed.

In figure 3.1.1, the multiple wake effect of a wind farm with 7 wind turbines is illustrated. Turbines T1, T2, and T3 are exposed to the free-stream velocity, while turbines T4, T5, and T6 experience a single wake effect. Turbine T7 encounters a multiple wake effect as it faces the wakes
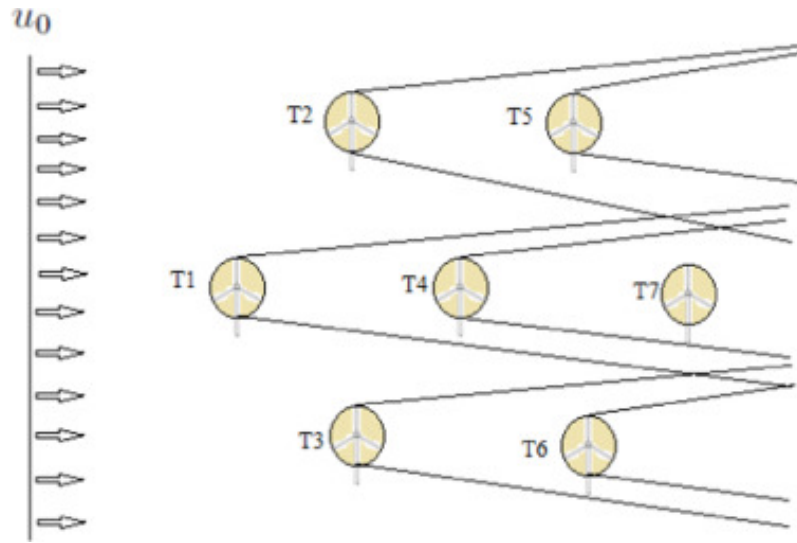
Figure 3.2: Multiple wake effect in wind farm.[49]

generated by two upstream turbines, T1 and T4.

The wind speed deficit at the location of turbine T7 is determined using equation 3.3. When a wind turbine is subject to multiple wake effects from upstream turbines, the resulting velocity, v_{i+1}, is calculated by equating the sum of the kinetic energy deficits of each wake to the kinetic energy deficit of the combined wake at that specific position.[49]

$$v_{i+1} = v_0 \cdot \left(1 - \sqrt{\sum_{i=1}^{N_t} \left(1 - \frac{v_i}{v_0} \right)^2} \right) \qquad (3.3)$$

Where, resorting to figure , v_0 represents the wind speed at, for example T1, v_i is the speed at this case present in T4 and it can be calculated using equation 3.2, and N_t is the number of turbines in question.

The Python script was developed to align the number of wind turbines present in a certain region in a rectangular shape, organized in columns and rows, similar to figure 3.1.1.

After following this procedure, it becomes feasible to determine the wind speed at the hub height of every turbine present in the wind farm. Wind speed is a crucial factor in accurately estimating the power generated by a wind farm. Following the documentation provided by *Windpowerlib*[54], two methods are available for calculating this value. *Windpowerlib* is a Python library that offers a comprehensive range of functions and classes specifically designed to determine the power output of wind turbines.

The first method involves using established tables that provide information about the power coefficient or coefficient of performance (Cp) curves for a diverse set of wind turbines. The Cp varies with the wind speed, and in this case, the wind speed varies by 1 m/s increments. To address the mismatch between wind speed values in tables and actual values, an interpolation method is employed to estimate the corresponding power coefficient value for a given wind speed. With this information and by resorting to formula 3.4[32] it becomes possible to calculate the hourly power

generated by the wind turbine. For that purpose, since wind density at the mean sea level is 1.225 kg/m^3 [39], and this value is widely used in wind power calculations, a constant air density ρ with this value is assumed.

$$P_{turbine} = \frac{1}{2}\rho A v^3 Cp \quad \text{,where} \quad A = \pi r^2 \tag{3.4}$$

In equation 3.4, A represents the sweep area of the blades of the wind turbine in m^2 where r is the radius of the wind turbine blades, and v represents the wind speed at the turbine's hub height. The tables mentioned in the previous paragraph also include data regarding the rotor diameter, rotor area, as well as the cut-in and cut-out speeds for each wind turbine model. These values define the range within which the wind turbine can effectively generate energy.

Ultimately, all the variables present in equation 3.4 are defined and with that information, it becomes attainable to calculate the hourly generated power by a wind turbine. By resorting to equation 3.5 and adopting the assumption of equal wind turbines, it becomes feasible to compute the power generated by the wind farm.

$$P_{farm} = \sum_{i=1}^{N_t} P_i \tag{3.5}$$

Where P_{farm} denotes the power generated by the wind farm in question, N_t is the number of wind turbines present on the wind farm and P_i represents the power of each wind turbine.

Alternatively, the second approach for calculating the power generated by the wind farm involves utilizing another set of existing tables that offer insights into the power output of various wind turbines based on the available wind speed, denominated by power curves. The existing data varies in 1 m/s increments, thus, an interpolation method is employed to estimate the corresponding power coefficient value that corresponds to the given wind speed, thereby addressing any disparities between the wind speed values in the tables and the actual values. This method solely relies on an interpolation technique to estimate the power generated by a wind turbine. Ultimately, the same interpolation methodology employed in the first method is used, also when calculating the power produced by the wind farm, indicated by the expression 3.5.

This method provides a comprehensive and detailed approach to calculate the power generated by the wind farm in question, for each hour, throughout a year. The resulting data, encompassing the power output at various time intervals, will serve as crucial input for the subsequent hydrogen model calculation, which will be thoroughly explained in the upcoming subchapter.

3.1.2 Hydrogen Model

In this subsection, the equation governing hydrogen production within the electrolyser will be introduced, as well a the equation used in the fuel cell. With this information, it becomes feasible to correctly employ these equations in the hydrogen production system, enabling the conduct of the case studies presented in the following chapter.

A study conducted by Bosio et al.[21] assessed the performance of several electrolysers, from different suppliers, including AELs and PEMELs, by comparing their efficiency. This study facilitated the forecasting of an average hydrogen flow rates across a broad spectrum of electrolyser's power consumption. These requisites ranged from levels below 1 Nm^3/h to a standard 4000 Nm^3/h of hydrogen. Accomplishing this goal involved conducting correlation analyses among different electrolysers and their corresponding performances.

The electrolysers under examination exhibited a wide range of sizes in terms of input power, spanning from as low as 1 kW, to approximately 10 MW. This research investigation also conclude that PEMELs generally exhibit higher electrical power requirements compared to other types, resulting in higher specific energy consumption, expressed as the electrical power required per unit of hydrogen flow rate.

The researchers analyzed the datasheets provided by the primary suppliers regarding these two types of electrolysers. In table 3.1 it is given a general insight of the type of electrolyser produced, by each manufacturer, that was present in this study.

Company	AELs	PEMEls
Areva H2Gen GmbH (France)		✗
Diamond Lite S.A. (Switzerland)		✗
Frames (The Netherlands)		✗
GreenHydrogen.dk Aps (Denmark)	✗	✗
H-Tec Systems GmbH (Germany)		✗
H2B2 (Spain)		✗
iGas energy GmbH (Germany)		✗
IHT S.A. (Switzerland)	✗	
ITM Power (United Kingdom)		✗
McPhy (France)	✗	✗
Nel (Norway)	✗	✗
Pure Energy Centre PEC (United Kingdom)	✗	✗
Thyssenkrupp Uhde Chlorine Engineers GmbH (Germany)	✗	✗
Siemens (Germany)		✗
Giner ELX (Massachusetts)		✗
Cummins (Ohio)	✗	✗
Proton On-Site (Connecticut)		✗
Teledyne Energy Systems (Maryland)		✗
Elchemtech (South Korea)		✗
Toshiba Energy Systems & Solutions (Japan)	✗	✗

Table 3.1: Presence of companies in the manufacturing of AELs and PEMEls technologies in the hydrogen industry.
OBS: The symbol "X" indicates the presence of the company in the respective category.

Table 3.1 presents a comparison between the manufacturing companies of AELs and PEMEls technologies. Among them, regarding the AELs, *IHT Industrie Haute Technologie S.A., Nel,* and *Thyssenkrupp Uhde Chlorine Engineers GmbH* specialize in manufacturing electrolysers of medium to large sizes, capable of producing hydrogen at flow rates of up to 4000 Nm^3/h. On the

other hand, *McPhy* offers a range of electrolysers with flow rates ranging from 0.4 Nm³/h to 800 Nm³/h, making it a more flexible supplier suitable for various hydrogen demand scenarios. To facilitate a more accurate and systematic comparison, different sets of hydrogen flow rates were identified, with increasing orders of magnitude.
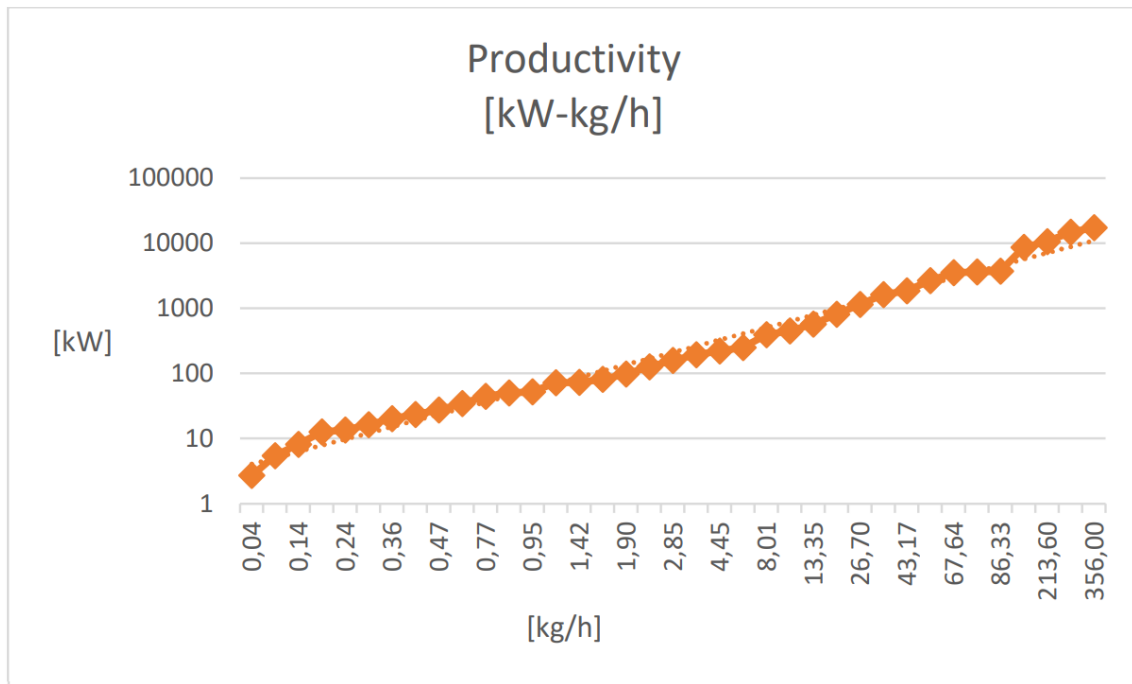
Figure 3.3: Variation of AELs capacity with hydrogen's mass production rate.[21]

Hydrogen Flow Rate [Nm³/h]	Flow Range [%]	Electrolyser Specific Energy Consumption [kWh/Nm³]	Electrolyser Specific Energy Consumption [kWh/kg]	Conversion Efficiency [%]
0.4 – 8.66	20 – 100	5.34	59.99	66.1
10 – 90	15 – 100	4.63	52.04	76.4
100 – 970	15 – 100	4.20	47.17	84.0
2000 – 4000	15 – 100	4.20	47.19	83.8

Table 3.2: Average values of the main Key Performance Indicators regarding AELs.[21]

As for the alkaline electrolysers, a technical analysis was conducted to compare the specifications provided in the datasheets of various suppliers. The number of suppliers offering PEM technologies is larger than those offering alkaline systems, as shown in table 3.1. The comparison of available PEMELs was carried out using the same methodology as previously described.

Through an analysis of the graphical representations illustrating the correlation between mass hydrogen production rate in kg/h and its associated electrical power in kW, on both AELs and
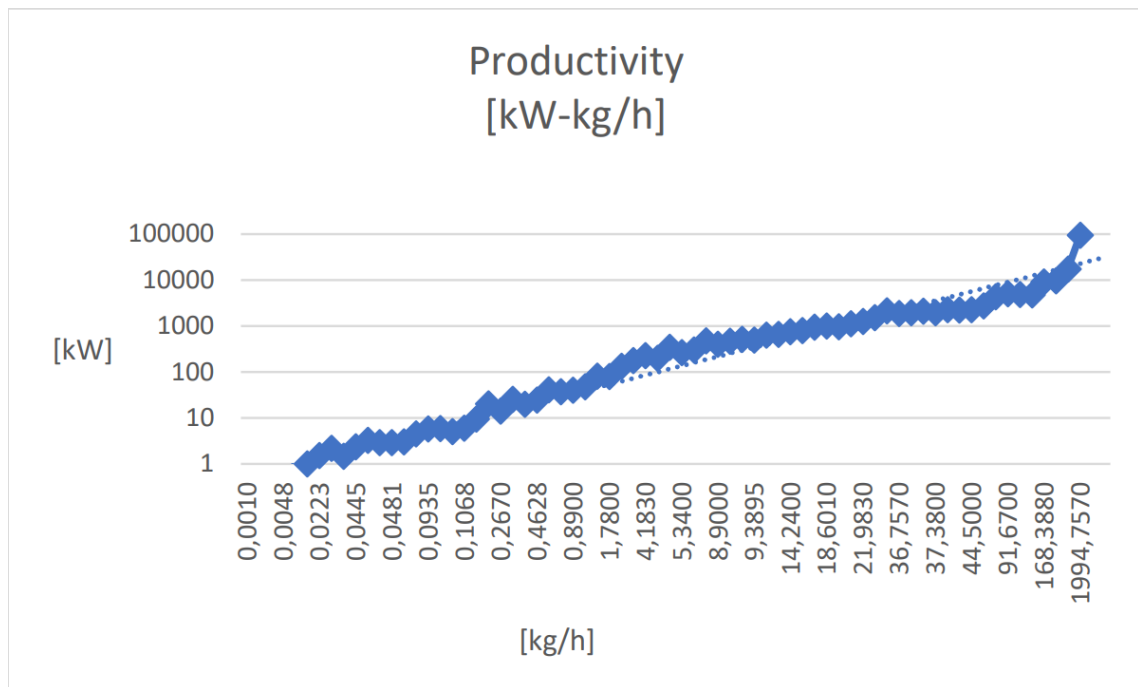
Figure 3.4: Variation of PEMELs capacity with hydrogen's mass production rate.[21]

PEMELs, represented in figure 3.3 and in figure 3.4, respectively, a linear pattern is unfold. The observed data unveils a discernible trend, characterized by a predominantly linear relationship. As the mass hydrogen production rate increases, there is a consistent rise in the required electrical power, without the appearance of any alarming spikes since there is not an outlier that requires an excessive request of power. This correlation, depicted by the smooth trajectory of the interpolating dashed line and its corresponding equation, underscores the efficiency of the examined technologies. Due to the observed linear pattern, it's reasonable to consider a constant specific energy consumption, as any errors resulting from this simplification are not substantial. To further reduce these discrepancies, a consistent specific energy consumption is applied for each range of hydrogen flow rate and electrolyser type, as shown in tables 3.2 and 3.3.

Based on this conclusion retrieved from the study conducted by Bosio et al.[21] and the formula proposed by K. Almutairi et al.[16], it becomes feasible to calculate the mass hydrogen production rate using the following equation:

$$\dot{m}_{H_2} = \frac{P_{EL}}{sec_{EL}} \cdot \eta rect \qquad (3.6)$$

Where $\dot{m}_{H_2}$ represents the hydrogen mass production rate in kg/h, P_E is the electrical power consumed by the electrolyser, in kW, $\eta rect$ represents the rectifier efficiency, which is the efficiency of the conversion of AC voltage to DC voltage. Since the voltage of the electrical power generated by the wind farm is AC, and the electrolyser operates with DC voltage, this conversion efficiency must be considered and, in this case, it was assumed to be 90%. The electrolyser specific energy consumption, in kWh/kg, is represented by sec_{EL} and its value is dependent on the

Hydrogen Flow Rate [Nm³/h]	Flow Range [%]	Electrolyser Specific Energy Consumption [kWh/Nm³]	Electrolyser Specific Energy Consumption [kWh/kg]	Conversion Efficiency [%]
0.011 – 6	0 – 100	5.72	64.5	63.3
10 – 78	0 – 100	4.90	55.2	72.9
100 – 580	0 – 100	4.62	52.0	76.3
1000 – 22413	10 – 100	4.53	50.9	77.7

Table 3.3: Average values of the main Key Performance Indicators regarding PEMELs.[21]

size of the electrolyser, which, in turn, determines the power associated to the electrolyser and the rate of hydrogen flow.

Based on equation 3.6, the calculation of the hydrogen mass production rate becomes crucial for determining the appropriate sizing of the hydrogen storage tank (HST) to accommodate the entire amount of hydrogen generated. The storage of hydrogen produced through water electrolysis involves storing it in a tank or transport it through a pipeline allowing the hydrogen collected to be further used to generated electricity, by resorting to a fuel cell. The amount of hydrogen stored in the tank is determined by a equation 3.7, as its rate of change depends on the mass flow entering and leaving the tank from the electrolyser and entering the fuel cell, respectively.

$$V_t^{\text{HST}} = V_{t-1}^{\text{HST}} + V_t^{\text{EL}} \cdot \eta comp - V_{t-1}^{\text{HST\_HM}} \tag{3.7}$$

Where V_t^{HST} and V_{t-1}^{HST} is the amount of hydrogen stored in the HST at time t and at time $t-1$, respectively, where t represents, in this case, the hourly variation of time. V_t^{EL} represents the hydrogen produced by the electrolyser in a certain hour and can be calculated resorting to equation 3.6. This equation allows to compute V_t^{HST} in Nm³ or kg, depending on the units of the electrolyser specific energy consumption, sec_{EL}, used for that purpose, since this variable can be expressed in kWh/Nm³ or kWh/kg. Ultimately, $V_{t-1}^{\text{HST\_HM}}$ is the amount of hydrogen sold from the HST to the hydrogen market at time $t-1$. This variable needs to be considered if the hydrogen storage is connected to a pipeline distribution due to the hydrogen output from the tank to the pipeline. However, if the hydrogen is not sold from the HST to the hydrogen market and, consequently, remains within the HST, this variable can be despised.

Additionally, a compressor should also be employed, depending also on the type of electrolyser available, in order to compress the hydrogen for storage and safety purposes. Thus, the efficiency of the compressor, $\eta comp$, becomes a relevant factor in the determination of the HST size since it directly affects the quantity of H_2 that can be produced. The energy previously solely allocated to the electrolyser will also be needed for the compressor. As a result of the utilization of energy to power the compressor, the available power for the electrolyser is diminished. This factor is of greater importance when using AELs, as PEMELs operate under higher pressures.

In this manner, hydrogen can serve as a means to store excess power generated by intermittent renewable sources such as wind. When the energy demand of the load exceeds the available energy generated by the wind power generation system, the fuel cell will be utilized to supplement the power supply and meet the load requirements.[42] Thus, fuel cells is utilized as the power module converting the stored hydrogen from the HST into electrical power and injecting it back into the power grid thus playing a significant role in facilitating the widespread adoption of clean renewable energy. In order to mathematically model this system, certain simplifications were made following the studies conducted by Nelson et al.[42] and Cerchio et al.[24]. Bearing this in mind, the governing equation can be expressed as:

$$P_{FC} = \dot{m}_{H_2} \cdot LHV_{H_2} \cdot \eta FC \tag{3.8}$$

Where P_{FC} is the electrical power fed to the fuel cell, in kW, $\dot{m}_{H_2}$ represents the hydrogen mass flow, expressed in kg/h, supplied to the fuel cell, LHV_{H_2} is the lower heating value of hydrogen, and its value is consider to be constant at 33 kWh/kg. The efficiency of the fuel cell, denoted as η_{FC}, is assumed to be constant and depends on the specific technology of the fuel cell employed, the variation of this value with the fuel cell technology is present in table 2.3.

In many instances, as the power demand, that will be produced the fuel cell, is frequently predetermined, and the desired parameter is the quantity of hydrogen flow required, denoted as $\dot{m}_{H_2}$, equation 3.8 can be reformulated into equation 3.9. This adaptation allows to determine the suitable hydrogen flow rate for a specific power demand within a given system.

$$\dot{m}_{H_2} = \frac{P_{FC}}{LHV_{H_2} \cdot \eta FC} \tag{3.9}$$

In the context of this scenario, when the fuel cell is operational, a diminution in the hydrogen reservoir within the HST ensues, due to the conversion of hydrogen reserves into electrical power. Thus, the HST reserves will diminish according to the following equation:

$$V_t^{HST} = V_{t-1}^{HST} - V_{H_2} \tag{3.10}$$

Where V_t^{HST} and V_{t-1}^{HST} is the amount of hydrogen stored in the HST at time t and at time $t-1$, respectively and the quantity of hydrogen required is denoted as V_{H_2}.

In this study, the fuel cell capacity was not considered a variable since the focus was primarily on understanding the influence of the electrolyser power capacity on the system, and for that purpose, the fuel cell capacity was left unspecified within a certain range.

3.2 Selection of Tools

Hydrogen production through the use of renewable energy sources, such as wind energy, is an important research area due to the increasing demand for sustainable energy sources. A model optimization is critical in enhancing the efficiency and effectiveness of hydrogen generation systems.

Hence, Python is a capable and versatile programming language that allows the manipulation of data resorting to extensive libraries for scientific computing, machine learning, and data analysis thus making it a suitable choice for this model application.

This programming language is well-suited for numerical computation and provides robust tools for data analysis and visualization, such as NumPy and Pandas, which enable efficient data processing and manipulation. These tools can help researchers understand the data patterns and relationships that are crucial for optimizing the hydrogen production model.

NumPy is a Python library for numerical computing in Python, providing a powerful array object that can handle large amounts of data efficiently. Its array interface facilitates vector programming and supports many numerical tools in the Python ecosystem. Another library built on NumPy is Pandas, which extends the array with labeling and an engine for structured and time-series data, such as the DataFrame and Series objects. Matplotlib is the core visualization library in Python that provides fine-grained control of graphics and offers a wide range of plotting tools and customization options. It is commonly used in combination with Pandas and NumPy for automated plotting of numerical data. Overall, these libraries work sequentially and can be used within the same analysis context, with data easily transferred between formats as needed.

Resorting to this programming language and aforementioned libraries, it is possible to import the data refer to the hourly variation of wind speed into a year and apply all the mathematical models mentioned above, with a strong capacity of data visualisation in order to better comprehend and study correlations between the inputs and outputs.

Chapter 4

Case Study

In this chapter, the case studies in question will be comprehensively explained, bridging the gap between mathematical modeling and methodology, and real-life practical applications. First, some wind and fuel cell projects that have been implemented worldwide will be reviewed. Next, the problem is formulated and, based on the aforementioned formulas, the wind farm production at a specific site is calculated. Finally, after analyzing the power generated,the two case studies will be implemented and examined.

4.1 Wind and Fuel Cell Projects

Over the years, numerous wind-to-hydrogen projects have been successfully demonstrated. These projects have showcased the potential of converting wind energy into hydrogen through various technologies. Additionally, there are currently several ongoing initiatives focused on power-to-gas and co-located wind and fuel cell installations worldwide.

National Renewable Energy Laboratory (NREL), in collaboration with partner Xcel Energy, is leading the $Wind_2H_2$ project in Boulder, Colorado. This project aims to enhance the efficiency of producing hydrogen from renewable resources, such as wind and photovoltaic arrays, on a large scale. The ultimate goal is to make hydrogen production competitive with traditional energy sources like coal, oil, and natural gas. The project connects wind turbines and PV arrays to electrolyser stacks, which are used to electrolyse water and produce hydrogen. The generated hydrogen is then compressed and stored at the on-site hydrogen fueling station. It can be utilized to power fuel cell electric vehicles or converted back to electricity using a hydrogen internal combustion engine or fuel cell. Thus, during peak-demand hours, the excess electricity can be fed back into the utility grid, further maximizing the utilization of renewable energy resources.[43]

In Japan, a wind-to-hydrogen project was initiated in April 2015 near Kabashima Island, located in Nagasaki Prefecture. This project utilizes large wind turbines to generate electricity offshore with a capacity of 2 MW. The generated electricity is transmitted to the island via an underwater cable. Any surplus electricity that is not immediately consumed is used to produce hydrogen, which is then stored for future use. During peak demand periods, the stored hydrogen can

be converted back into electricity or can be transported to remote islands, providing a continuous and reliable power supply to those areas.[14]

Another example, Project HAEOLUS, situated in Europe, focuses on integrating a 2.5 MW PEM electrolyser into a remote wind farm in northern Norway. The aim is to showcase the benefits of combining wind power with hydrogen production using the PEMEL. Afterwards, hydrogen is distributed through a 100 kW PEM fuel cell for various applications. This integration enhances flexibility, grid integration, and economic profitability due to the implementation of a remote monitoring system, ensuring efficient operation.[63]

4.2   Problem formulation

The power generated from a wind farm is typically exported to the electricity market, although it can also be utilized to meet the power demand of different entities such as buildings, factories, or even entire cities. The wind's kinetic energy is one of the most dominant aspects in wind power generation. However, wind power generation is characterized by its variability due to the continuously changing value and direction of the wind. This variability leads to fluctuations in power output as the energy generation is proportional to the wind speed.

However, due to this wind intermittent regime, the energy produced from the wind farm occasionally overcomes the electricity that the grid demands, resulting on a loss and waste of energy. Although, this obstacle can be overcome by redirecting the excess of energy to an electrolyser in order to produce hydrogen that can later be compressed and stored in a hydrogen storage tank or even fed directly to a pipeline distribution. Bearing this in mind, hydrogen can be produced whenever there is an excess of energy resources and reconverted to serve as backup during limited resources. For that purpose, the stored hydrogen is subsequently fed into a fuel cell where it combines with oxygen to produce water and generate electricity. This process helps bridge the gap in electricity supply during periods of lower wind speeds. This process allows renewable energy to be integrated into the grid using hydrogen as the storage system.

In conclusion, the system analysed, under these circumstances, consists on a wind farm that is composed by several wind turbines that generate power in order to supply the demand, an electrolyser to convert energy into hydrogen, a HST to store the hydrogen produced and a fuel cell able to reconvert hydrogen into energy, in order to meet all the parameters discussed above.

The wind-electrolytic hydrogen storage system is not solely reliant on wind energy from the farm. There are instances when the hydrogen storage tank may be empty, resulting in an inability to provide hydrogen to the fuel cell and meet the energy demand. This can happen when the power generated by the wind farm falls short of the power required by the grid, and the hydrogen reserves are either low or depleted.

Such scenarios can arise if the consumption rate of hydrogen is too high for a given period, leading to a gradual decline in the hydrogen reserves. To meet the energy demand during these situations, it becomes necessary to purchase electricity from the grid in order to compensate for the power that cannot be supplied by the wind farm at that particular time.

The combination of wind power and hydrogen technologies have given the wind industry new directions and opportunities since it is possible to convert extra wind energy into hydrogen with efficiency, creating a useful energy source that can be stored and used as needed. This strategy improves the overall efficiency and sustainability of the wind sector by maximizing the use of renewable energy sources and ensuring that no wind power is lost during periods of high demand.

From a more economical perspective, regarding profit and selling potential, wind farm owners have the opportunity to optimize their revenue by strategically selling the generated power to the electricity market. The inherent variability of electricity prices provides a chance for wind farm operators to engage in price arbitrage, where surplus energy can be stored during periods of low prices and later sold during periods of higher prices. By adopting this approach, wind farm owners can maximize their earnings. The successful implementation of price arbitrage in wind farms heavily relies on the proper sizing and selection of electrical equipment and HSTs as its volume should be carefully chosen to store adequate hydrogen until it can be sold profitably at times of high prices. However, it is also possible to employ a system of hydrogen deployment into pipelines, enabling its transportation without the need for carrying HSTs.

The competitiveness of this combined wind energy and hydrogen conversion system approach its directly dependant on the optimization and planning of the facility. Oversizing the electrical equipment or the hydrogen tank can lead to unnecessary costs, while undersizing may result in missed opportunities to maximize profits. Therefore, research, modeling and implementation are necessary to fully harness the potential benefits of this renewable energy solution, benefiting wind farm owners and contributing to a more economically viable and sustainable electricity market.

Figure 4.1 represents a schematic that summarizes the illustrates the operational approach relative to the working operation of a wind farm that uses a fuel cell to fulfill energy requirements. This system comprises a fuel cell and an electrolyser, both interconnected with the wind farm.

The aim of the presented model is to fulfill the energy needs of a hypothetical institution, company or even small city. It is noteworthy that, the power demand under consideration it is not a fixed value and that, for the purpose of this study, the value chosen for this parameter, is the power output that this specific wind farm could have potentially generated in the year of 2021. To achieve this objective, a preliminary assessment is undertaken to determine whether the current power generation from the wind farm is adequate to satisfy the prevailing demand. If the wind farm's output falls short, the deficit is rectified by procuring the requisite energy from an external source.

Initially, the focus will be on investigating the most favorable scenario for the wind farm, where the energy generated surpasses the present demand creating an energy excess. In such instances, three potential courses of action can be pursued subsequently. It is worth noting that this approach deviates from conventional methods, as the surplus energy will be harnessed not by conventional battery storage, but by utilizing hydrogen as an energy storage medium, which can later be harnessed to generate electricity.

For this purpose, the concept of production capacity dynamic range must be introduced. In essence, the dynamic range signifies the flexibility of the electrolyser to adapt its hydrogen pro-
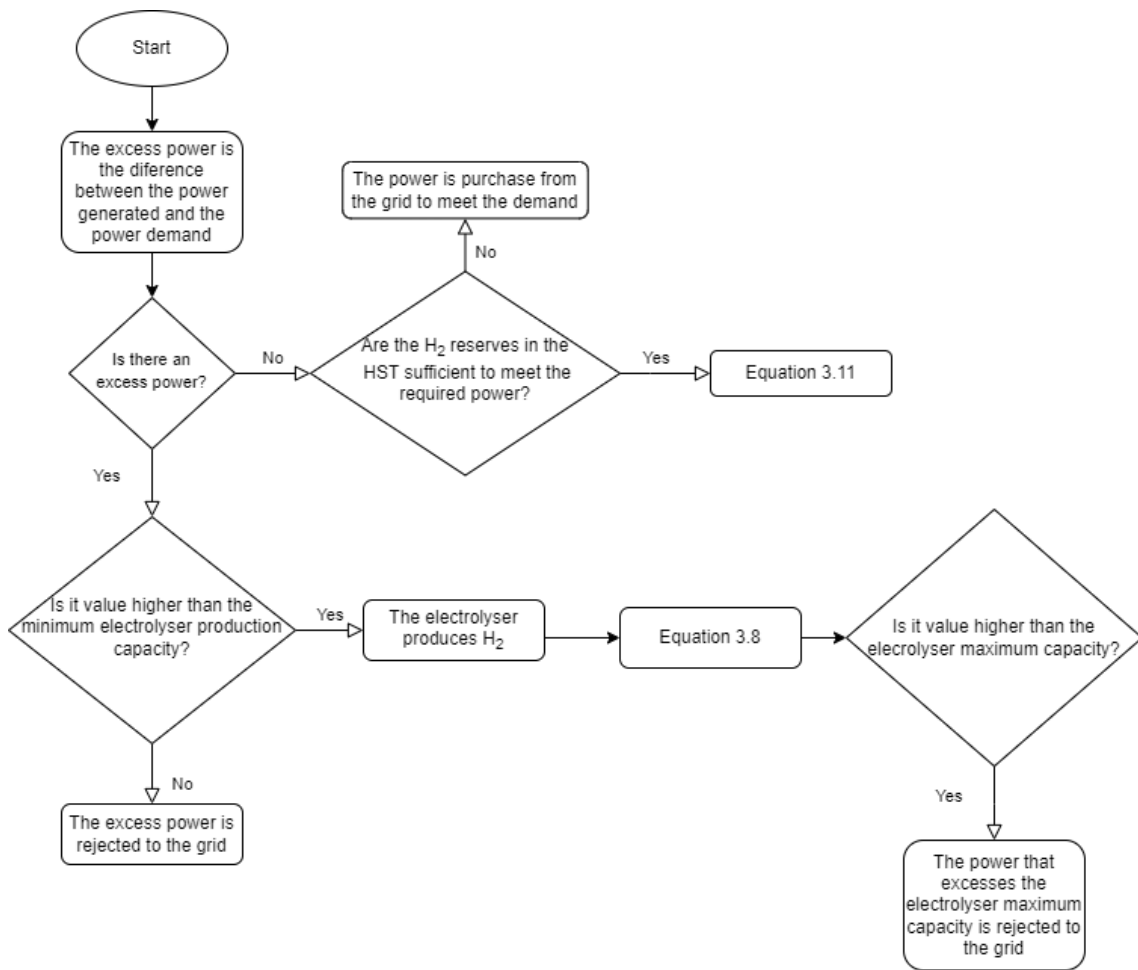
Figure 4.1: Flowchart explaining the first case.

duction output according to variations in the energy input. By establishing an operational window range of its rated capacity, the electrolyser is expected to effectively respond to fluctuations in energy availability while producing hydrogen efficiently. Usually, from the available literature this span its adjusted between 15% to 100% regarding alkaline electrolysers. On the other hand, it is notable that the PEM electrolyser are more versatile in this aspect, since they do not necessitate a minimum power input to facilitate their operation. This information is supported by table 2.2.

One of the aforementioned scenarios is characterized by the surplus power not exceeding 15% of the rated power of the electrolyser. Consequently, the production of hydrogen becomes unfeasible in this context. With the inability to store this excess energy, the alternative course of action involves channeling it into the grid. Nevertheless, when the power demand has already been satisfied and the surplus energy falls within the operational capacity of the electrolyser, the prospect of hydrogen production becomes viable. In this operational context, equation 3.7 will be employed to compute the volume of the reservoir at the specific time. For this purpose, it is crucial to resort to equation 3.4 to assess the amount of hydrogen generated. This equation, as elaborated upon, in chapter 3, relies on the constant value of sec_{EL}, which is dependent upon the type of electrolyser

in question.

Specifically, in the case of AEL, the electrolyser's specific energy consumption stands at 47.17 kWh/kg, considering a hydrogen flow rate ranging from 100 to 970 Nm³/h, as evidenced in table 3.2. However, for hydrogen flow rates higher than 100 Nm³/h, the specific energy consumption can be considered as constant.

Regarding the PEMEL, its specific energy consumption stands at 52 or 50.9 kWh/kg , considering a hydrogen flow rate ranging from 100 to 580 Nm³/h or 1000 to 22413 Nm³/h, respectively, as considered in table 3.3

From the analysis conducted above, it is possible to conclude that the PEMEL is more suitable to work under fluctuating power supply due to the fact that the transportation of protons across the membrane responds quickly to fluctuating power supplies. Therefore, in this case, the use of a PEMEL is more appropriate. Additionally, its production capacity range encompasses all the power that can be supplied to it until it reaches its maximum capacity. Compared to the AEL, this is a better approach since there would be no energy loss to the grid due to not meeting the minimum power required for hydrogen production.

In this context, $V_{t-1}^{\text{HST\_HM}}$ is presumed to be null, given that this particular circumstance revolves around a reservoir where the possibility of selling hydrogen to the market is not taken into account and consequently, all the produced hydrogen remains in the reservoir.

The final scenario within this context pertains to situations where the surplus power surpasses the maximum capacity of the electrolyser, rendering it incapable of utilizing the entirety of the surplus power. Consequently, the excess power beyond the electrolyser's capacity is directed into the grid, as storage is unattainable under these circumstances.

Having examined all instances characterized by an energy surplus, it is now crucial to analyze scenarios where a power deficit emerges. This phenomenon occurs when the wind farm cannot single-handedly adequately meet the demand. It is precisely for such cases that the previously generated hydrogen comes into play. Given the insufficiency of energy generated by the wind farm to fulfill the demand, an alternate approach is adopted. This entails harnessing the potential of the fuel cell while simultaneously utilizing the hydrogen stored within the reservoir.

To achieve this objective, an evaluation is necessary to determine whether, at the specific time under consideration, an adequate quantity of hydrogen resides within the reservoir. This hydrogen is intended to power the fuel cell and, along with the power generated by the wind farm, meet the prevailing demand. In pursuit of this goal, the hydrogen mass flow rate supplied to the fuel cell stands as a pivotal parameter, that is predetermined by the necessary electrical power required as output from the fuel cell, as elucidated by equation 3.9. As a result of this process, the hydrogen reserves within the HST experience depletion, as the composition of the HST now comprises the pre-existing hydrogen content minus the portion expended to satisfy the power requirements. If this calculated value proves insufficient compared to the hydrogen available within the reservoir, the sole recourse entails purchasing electricity from the grid in order to meet the demand since that it is assumed that the plant is connected to the electrical grid with the possibility of selling

and purchasing electrical energy. It is important to underscore that this alternative is regarded as a last resort, since the objective of this system is to achieve self-sufficiency.

In contrast to the previous scenario, the second case focus exclusively in hydrogen production, with surplus electricity being directly sold to the grid. Rather, the emphasis lies in strategic commercialization of the produced hydrogen as a clean transportation fuel or a valuable industrial commodity. The electrolyser, renowned for its inherent flexibility, assumes a important role in supporting and optimizing the wind farm's operations.

By adopting this configuration, capital costs are effectively curtailed, as the need for a fuel cell system is eliminated, since that the conversion of hydrogen into electricity is no longer required. By focusing efforts solely on hydrogen production, it allows the wind farm to capitalize on the demand for environmentally friendly hydrogen applications, which encompasses its deployment as a green transportation fuel and its utility in diverse industrial processes.

By relinquishing electricity sales in favor of high-value hydrogen production, the wind farm actively contributes to a diversified and sustainable energy landscape while simultaneously optimizing its cost structure. For this purpose, it is crucial to consider that the selling price of hydrogen is significantly higher than that of electricity, given its expensive production process and the current scarcity of hydrogen production and adoption worldwide. While hydrogen's growth as a viable energy source is noticeable, it is evident that sustainable energy derived from hydrogen is still in its early stages of widespread adoption. Consequently, there is a limited number of companies currently in need of substantial hydrogen quantities. Nevertheless, this study will assume that are companies that are interested and that necessitates a steady, continuous, and annual supply of hydrogen.

As the first case is more theoretical and engineering-focused, the second case was introduced to provide insight into the hydrogen market pricing relatively to the components required for its production, specifically the electrolyser and the HST. The objective here is to offer an economic perspective and also understand the variation in the investment payback period for a model where different sizes of electrolyser units are studied across a range of hydrogen selling prices. Additionally, the aim is to analyze the conditions that would result in higher profits for hydrogen sales from the wind farm in question.

Initially, to ensure the accurate utilization and interpretation of the hydrogen model, an evaluation of the wind farm's power output is essential. To accomplish this, the mathematical model pertaining to the wind farm, as detailed in Section 3.1.1, is employed.

This Python-based model is designed as a versatile framework, and has as its primary aim is to provide the most precise power generation predictions attainable. This is achieved by considering the wind speed's hourly variability within a year and accounting for various influencing factors. These factors encompass wind turbine variability, turbine count, wake effects, and other pertinent specifications. To facilitate this, data, such as that obtainable from sources such as the *POWER Data Access Viewer*, is utilized. This data permits the retrieval of wind speed readings from two distinct altitudes, that is essential to predict the wind speed at the turbine's hub height. This implies that due to the capabilities of the referenced software to access wind data from any location

worldwide, the model serves as a valuable tool to comprehensively assess the power generation potential within a specific geographical area.

4.3   Wind Production at Site

The methodology commences with an examination of potential wind farm locations. This selection process involved a comprehensive search to identify regions with substantial wind speed potential, primarily focusing on existing wind farms in Portugal, where the feasibility and practicality of wind turbine installation are well-established. For this study, the chosen location was Arada/Montemuro. The Arada/Montemuro wind farm is situated in the northern region of Continental Portugal, specifically within the Viseu district. This expansive wind farm comprises four distinct wind subfarms, strategically positioned across the municipalities of Cinfães, Castro Daire, and São Pedro do Sul.[11] This choice was not made due to its specific geographic attributes, but rather as a pragmatic decision to fed the model with actual data from a tangible region. Moreover, this local serves to exemplify the feasibility of constructing a wind farm with a commendable power production capacity.

To conduct an in-depth analysis of power production at the designated site, wind speed data from the year of 2022 was extracted from the *POWER* software in a specific location with coordinates *40°57'49.3"N 7°56'30.1"W*. One of the most preeminent factors that significantly influence on-site production is the wind speed profile, thus, for analysing this factor, an indispensable component of the study encompasses the analysis of wind direction.

Wind roses serve as indispensable tools for conducting a comprehensive analysis of wind direction, since they show prevailing wind direction which is crucial in the placement of wind turbines, exerting a direct influence on their efficiency and overall performance. The optimal operation of turbines is achieved when they are oriented into the prevailing wind, enabling them to capture the maximum available energy and to ensure a efficient operation. This underscores the indispensable roles that wind resource assessments and meticulous planning assume in ascertaining the most advantageous orientations for wind turbines.

Figure 4.2 displays the wind rose corresponding to the prevailing winds at the location under consideration and it is important to refer that the unit of range of wind speeds present is in m/s. An examination of this image reveals that the predominant wind direction originates from the south and means that the wind turbine should be facing this direction. Nevertheless, it is important to note that the northern and western regions also experience significant wind speeds. This considerable variation in wind direction poses potential challenges for wind turbines and, consequently, for the entire wind farm.

The substantial diversity in wind speed direction can lead to increased structural stress on wind turbines, primarily from the high speed wind that it is not contributing to power generation. This heightened stress may adversely impact the longevity of the turbines, potentially necessitating maintenance sooner than anticipated.
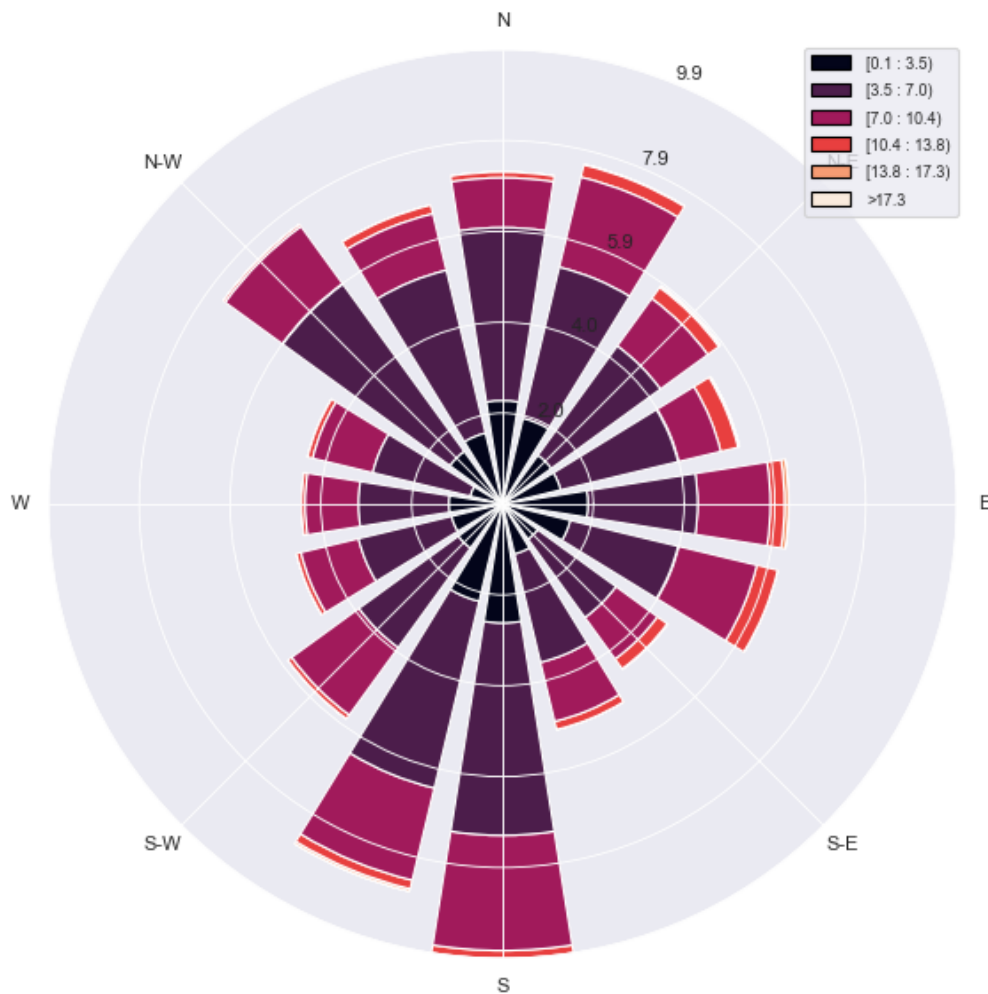
Figure 4.2: Wind rose corresponding to the wind at the location under consideration.

To predict power production levels accurately, an in-depth analysis of the wind profile is imperative. This analysis employs a histogram to establish the frequency of occurrence for each wind speed, which is then aligned with the Weibull distribution of the wind. The Weibull distribution is a useful tool in estimating the duration for which the wind sustains a particular velocity, offering a probability density function for each wind speed. Figure 4.3 reveals that, for this site, the most frequently recorded wind speed is approximately in the middle of 5 and 7 m/s that reveals to be true since the Weibull scale factor indicates an average wind speed of 6.2. Moreover, the curve exhibits a relatively narrow distribution, with 12.5 m/s serving as a reasonable upper limit for registered wind speeds. This observation aligns with the Weibull scale factor of 2.25, indicating that the wind speed data at this location exhibits moderate variability reflecting a mix of lower and higher wind speeds.
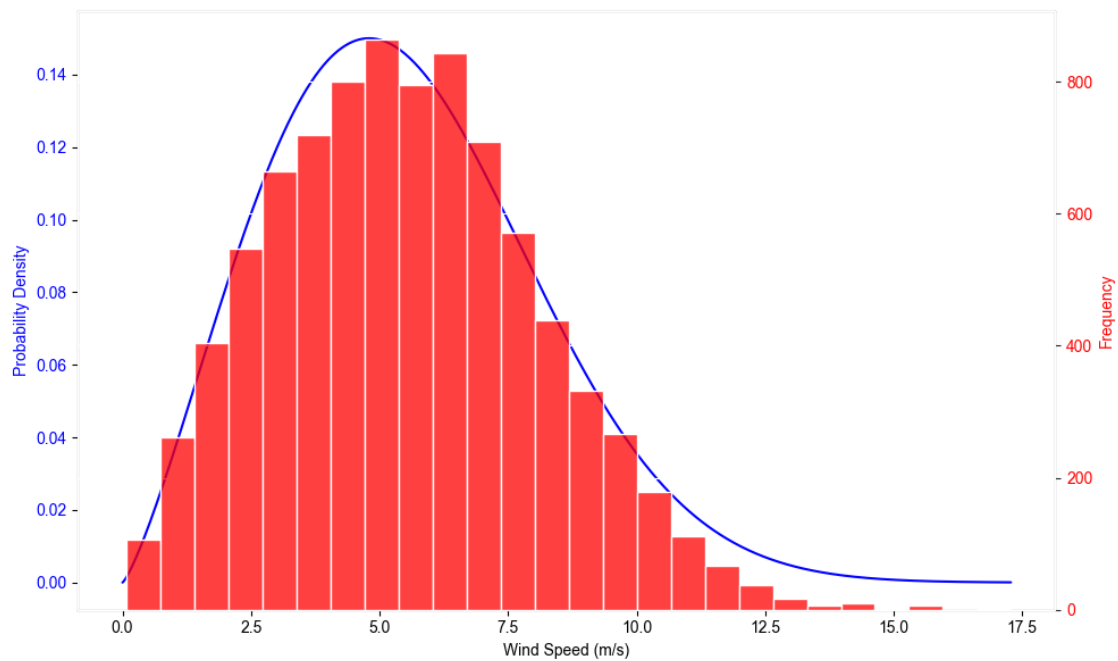
Figure 4.3: Wind speed frequency and probability variation.

With this data is possible to achieve the probability density function for each wind speed within the interval relative to the power curve that corresponds to the chosen turbine model and it becomes feasible to approximate the Annual Energy Production (AEP) for the specific model. For this purpose, equation is used to predict the average power production within an hour, and formula allows to estimate what would be the annual power production from a single turbine at site by considering that the turbine produces that amount of power at every hour of the year. The AEP estimation is a very important factor within the context of wind resource assessment, aiding in the determination of the site's suitability for wind energy generation since it gives an estimation on the power that could be generated by the wind farm at that specific site.

Subsequently, the following step involves the evaluation and selection of a wind turbine model that best aligns with the acquired dataset. While price considerations are not currently factored in, an initial approach involves creating a system that compares the annual power output of various wind turbines sourced from a comprehensive database with the aim of identifying the turbine with the most favorable performance characteristic.

However, this approach demonstrated limitations by potentially leading to the selection of a specific model that is consistently selected for every site and for practically every wind profiles. The explanation for this is that power output is significantly influenced by the wind speed, as evident in equation 3.4, which is determined at the turbine's hub height. As speed increases with height, as explained by equation 2.2, it directly affects power generation. Furthermore, as turbine size increases, the blades also follow suit, resulting in a larger swept area. Thus, since this turbine has an increased hub height and rotor diameter, it will consistently be more advantageous in generating more power at the same location. To address this issue, a comparative study involving

turbines from two different manufacturers was conducted.

The selected turbines were deliberately chosen with exact same hub height. This strategic decision was employed with the aim of minimizing the influence of wind velocity variations and ensure that each turbine experiences the same wind speed at hub height. If the discrepancies in swept blade area were also disregarded, the focus primarily hones in on the power coefficient curve since it is a crucial parameter for evaluating wind turbine performance. Additionally, to ensure an unbiased study of these three wind turbines, it is imperative that their nominal power values are closely matched. The nominal power of a turbine is defined as the maximum output power that can be generated under specific operating conditions and serves as a reference point for the turbine's performance and capacity planning.

After a reliant search of a database containing wind turbine data, the selected turbines were the SWT130/3300 produced by *Siemens*, the N131/3300 manufactured by *Nordex*, and the GE130/3200 fabricated by *GE Wind*. Here, the initial acronyms represent the respective turbine manufacturers, followed by the rotor diameter in meters, and the nominal power in kW, denoted after the slash. The current data information is available in the *Windpowerlib Documentation*[54].
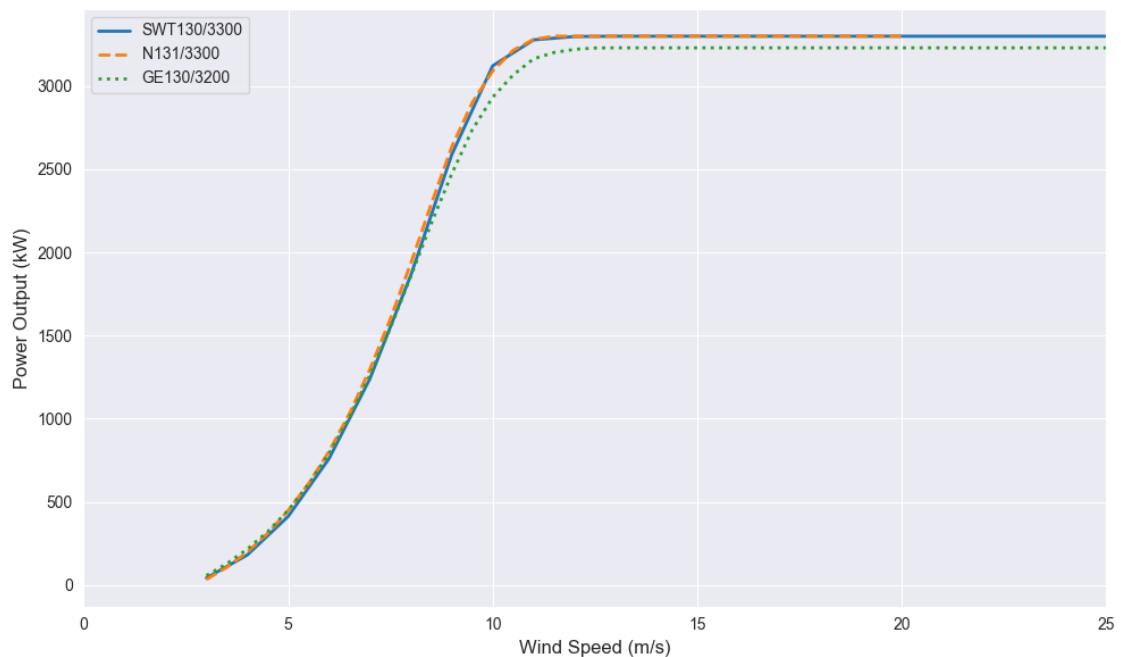

Figure 4.4: Power curves associated to the wind turbines in study.

Figure 4.4 contains the graphical representations that illustrate the power curves that are linked to the wind turbines currently being examined in this study. Upon examining the provided illustration, it becomes apparent that the curves exhibit a remarkably similar trajectory. The primary distinction emerges in the context of the GE130/3200 turbine, which showcases a lower power level due to its reduced nominal power. Additionally, a variation is evident in the cut-out speeds, where the N131/3300 turbine features a cut-out speed of 20 m/s, diverging from the other two

turbines which possess a cut-out speed of 25 m/s. However as the wind speed rarely exceeds this limit, the importance of this factor for this site is minimal.

Turbine Type	Nominal Power (kW)	Rotor Diameter (m)	Rotor Area (m^2)	Hub Height (m)	Annual Power Production (MWh)
SWT130/3300	3300	130	13272	135	7776
N131/3300	3200	131	13477	134	7862
GE130/3200	3200	130	13272	134	7731

Table 4.1: Technical specifications of wind turbines.

Table 4.1 provides an overview of the aforementioned wind turbines, including key characteristics and the anticipated annual power output for each turbine. This parameter is of great significance in the decision-making process for selecting the most suitable wind turbine. Furthermore, the specific hub height utilized in the calculations corresponds to the measurement provided by the turbine manufacturing company, as it is predetermined by the turbine manufacturer. Hence, it should be noted that the hub height of the SWT130/3300 turbine does not precisely align with the hub height of the other turbines.

The power output of the wind turbines was computed by applying equation 3.4. To achieve this, the known hub height serves as a vital parameter for employing the wind shear equation 2.2, thereby obtaining an estimated wind speed at that specific height. Bearing this in mind, all the parameters relevant to equation 3.4, that define power generated by the turbine, can be determined. The sole parameter that necessitates determination is the power coefficient. Extracted from the power coefficient curve, this curve illustrates how the coefficient values vary with wind speed for each turbine, spanning from the turbine's cut-in speed to its cut-out speed. However, it is important to note that the known power coefficient values are typically available in wind speed increments occurring at intervals of 0.5 m/s or 1 m/s, contingent upon the turbine-specific data.

In nearly all instances, the wind speed aligns within a range defined by two known power coefficients, which correspond to established wind speeds. Consequently, the approach employed to determine the C_p involves interpolation, utilizing the current speed and the speed marking the boundary of the given interval, as outlined in the following linear interpolation formula:

$$C_p = C_{p1} + \frac{(v - v_1) \cdot (C_{p2} - C_{p1})}{v_2 - v_1} \tag{4.1}$$

Were, C_p is the interpolated power coefficient at the current wind speed v, and C_{p1} and C_{p2} are the known power coefficients corresponding to wind speeds v_1 and v_2, respectively. v_1 and v_2 are the established wind speeds marking the boundary of the given interval.

Given that the speed values at the site, exhibit hourly variations, this parameter also follows this pattern. This signifies that power generation will be calculated for each hour throughout the

year. With this information, it is also possible to compute the total annual power production, by applying a methodology that involves aggregating the power generated across all hourly intervals.

Examining the last column of table 4.1, it becomes evident that the N131/3300 turbine achieved the highest production when compared with the other two, even though that the power difference is not that notorious. As a result, this turbine has been selected to populate the hypothetical wind farm.

Currently, the subsequent stage entails computing the power that would be generated within a wind farm. As elaborated in chapter 3.1.1, this process necessitates a comprehensive evaluation of wake effects on wind speed, taking into consideration the arrangement of turbines within the wind farm. Regrettably, these wake effects have the potential to diminish the overall power output of the farm due to the wind speed decay induced by these effects.

In this analysis, it was assumed that the wind farm consists of eight wind turbines. This configuration provides the opportunity to investigate a scenario that outlines both wake models. The wind speed of the turbines in the second row, where a linearly expanding wake is assumed, followed the Jensen wake model described by equation 3.2. In subsequent rows, the wind is subjected to multiple wake effects from upstream turbines where the equation governing wind speed in these scenarios is represented by equation 3.3.

Subsequently, the procedure outlined above, following the calculation of wind speeds for each turbine and accounting for the wake effects, was implemented. To accurately assess the total power generation, the power generated by each turbine was calculated using the wind speed data previously obtained and the sum of the power generated by all turbines present in the farm totalled the power generation of the wind farm, as described in equation 3.5.

To analyze the variation in power generation throughout the year, the utilization of a boxplot as demonstrated in figure 4.5 was used. This graph serves as a valuable visual tool for scrutinizing the wind farm's power generation patterns throughout the year. These box-and-whisker plots provide key insights into various aspects, including central tendencies, variability, and the presence of potential outliers in power output.

Upon analyzing figure 4.5 and considering factors such as the position of the median, the length of the box, and the existence of outliers, discernible patterns emerge. It becomes evident that the months falling in the middle of the year, spanning from April to August, exhibit lower power generation levels. This is due to less frequent occurrences of higher wind speeds, leading to the presence of more outliers. Conversely, the remaining months align with the winter season, where wind velocities tend to be higher. This, in turn, directly corresponds to increased power generation output in the wind farm during these months, as reflected in the boxplot.

4.4   Case 1 - Fuel Cell - Hydrogen as a energy storage system

In this section, a practical evaluation of the case previously theorized and formulated will be conducted. The objective is to assess the potential implementation of a power to hydrogen system,
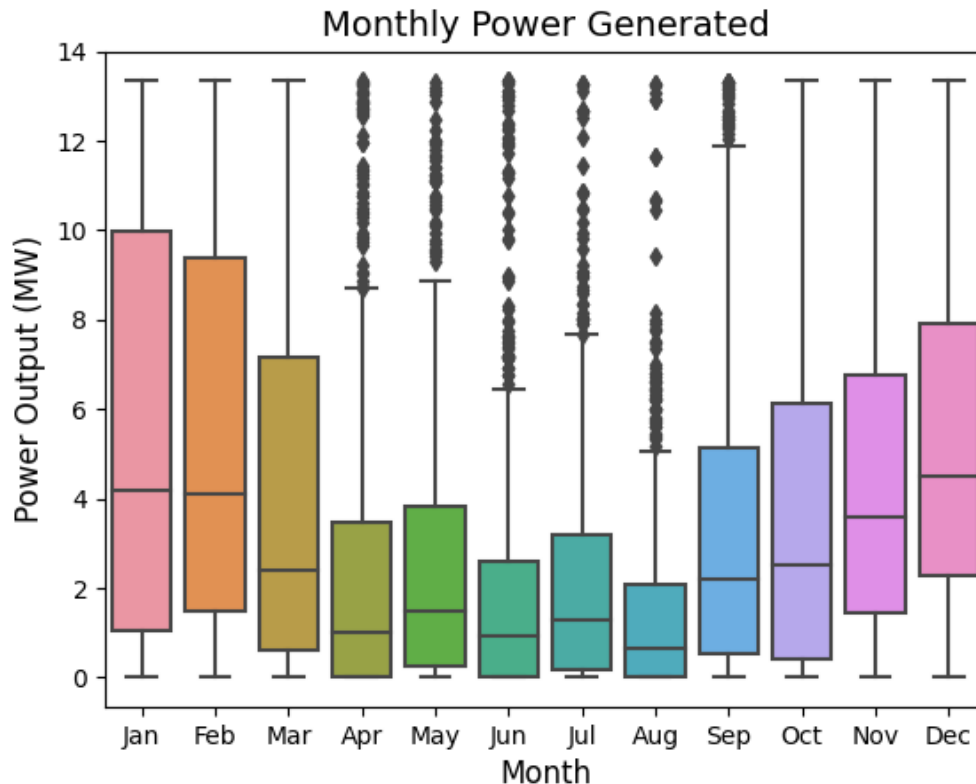
Figure 4.5: Monthly power generated at the wind farm.

consisting of an electrolyser and a HST, as well as a fuel cell to reconvert the hydrogen into power, to assist in meeting energy demand.

Figure 4.6 provides a graphical representation of the weekly variation in power output from the wind farm compared to the selected power demand. These values fluctuate from week to week and represent the mean power production or power demand for each specific week. Regarding the power demand, it was calculated using the same procedure as mentioned earlier, however the wind speed data used was from the year 2021. The choice of this year was arbitrary and served as a basis for comparison to effectively employ and test the model, ultimately leading to conclusions. Clearly, the wind profiles for the two selected years were dissimilar, as evidenced by the significant disparities in the power graphs. This suggests that predicting wind profile patterns at the site in question would be a challenging task.

The observed figure also illustrates the power discrepancy, which represents the difference between the power output and the demand. Negative values indicate a power deficit when the demand exceeds the power generated however positive values represent a power surplus when the power generated surpasses the power demand. The analysis of the graph reveals that these values fluctuate between positive and negative, with a noticeable peak occurring in the middle of October and November. This peak likely indicates a depletion of hydrogen reserves, necessitating the system to purchase electricity from the grid.
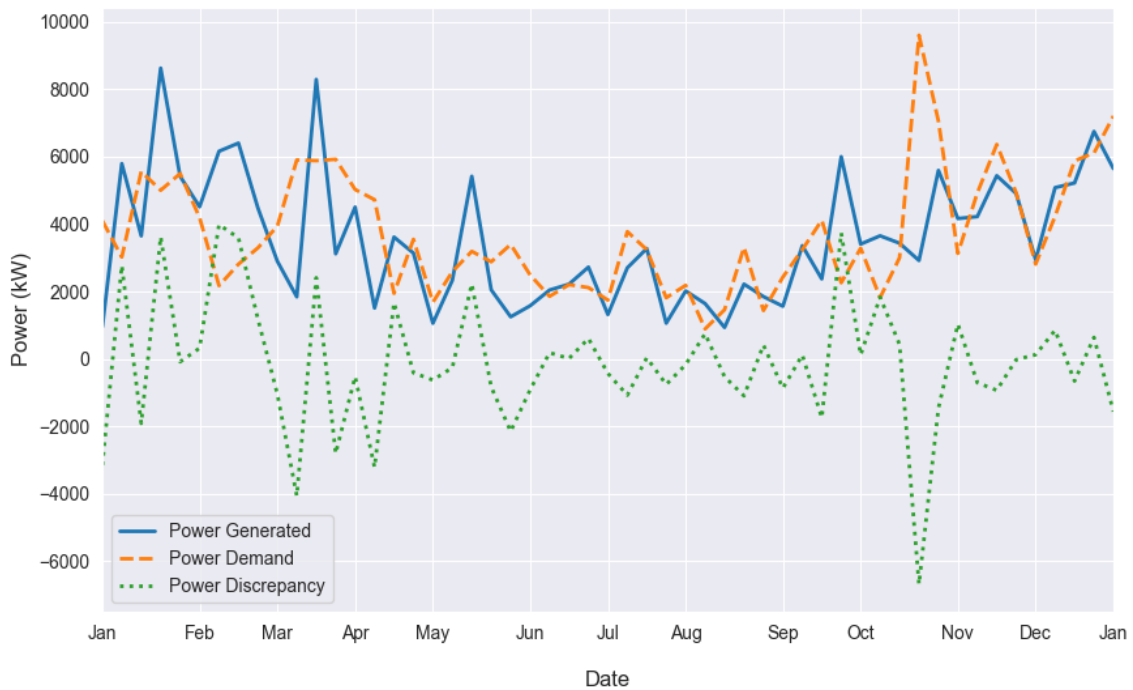
Figure 4.6: Disparity between the power generated and the power demand at the wind farm.

The model, as summarized in the flowchart presented in Figure 4.1 and explained in Chapter 4.2, takes as inputs the power generated and the power demand and deliver as outputs, the power that needs to be purchased from the grid and the volume of the HST required to store all the hydrogen, in order to meet the demand. Figure 4.7 illustrates the power consumed from the grid as its annual hourly mean value, while the volume of the HST is represented as the maximum volume of hydrogen required to store all the hydrogen produced during that year. The size of the electrolyser has a significant impact on this matter, as it affects the quantity of hydrogen produced, which subsequently alters the power needed from the grid.

To study the effect of the electrolyser's size on these two output factors, values for this parameter were assumed across a range of electrolyser sizes, spanning from 500 kW to 10 000 kW.

Firstly, it's important to note that the HST is measured in Nm^3, but it was initially calculated using equation 3.6, which provides the output in kilograms. Then, with reference to the values present in table 3.2 that were obtained in the study conducted by Bosio et al[21], it becomes feasible to obtain the hydrogen density, that will be considered, by dividing the electrolyser's specific energy consumption in kWh/Nm^3 and kWh/kg. Multiplying this value by the maximum hydrogen mass obtained within the HST, H_2max, allows the estimation of the HST volume. This process can be summarized in equation 4.2.

$$HST = H_2max \cdot \frac{4.2\,\text{kWh/kg}}{47.18\,\text{kWh/Nm}^3} = H_2max \cdot 0.089\,\text{Nm}^3\text{/kg} \tag{4.2}$$

By directing the attention to the values displayed on the right y-axis, it becomes evident that they encompass a notably wide range of values, and these values tend to rise with an increase in
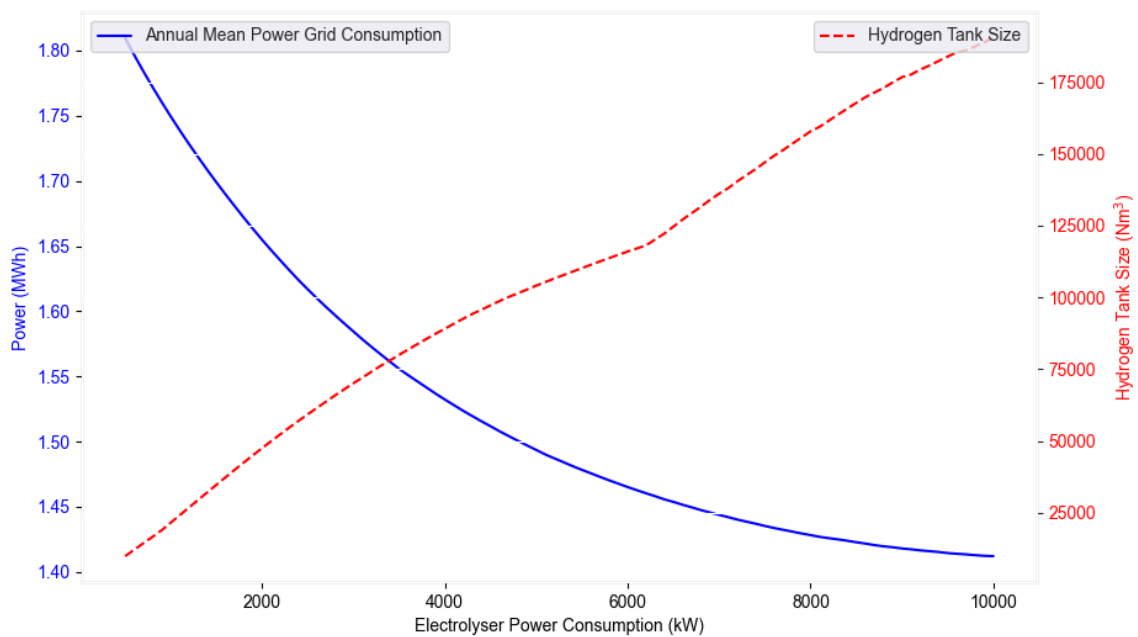
Figure 4.7: Comparison between the annual hourly mean power grid consumption and hydrogen tank size for a range of electrolysers.

electrolyser capacity. Assuming a linear trend, it can be observed that for every additional kW of electrolyser capacity, there is an associated increase of 2098 Nm^3 in the required storage space within the HST. As illustrated, this storage demand escalates considerably with the electrolyser's power capacity.

Conversely, focusing now in the left y-axis, the amplitude of the power bought from the grid does not appear to be significantly affected, as evidenced by the 400 kWh decrease in power consumption. However, it is crucial to emphasize that this value represents an hourly mean since in order to assess this on an annual scale, it would need to be multiplied by the total number of hours in a year. Power consumption fluctuates, occasionally reaching zero or levels much superior than the mean. In a conventional setup, without utilizing hydrogen as an energy storage medium, the estimated annual power grid consumption would be 2.78 MWh. With the introduction of the hydrogen-based solution, this consumption could be reduced by approximately 1 MWh. This reduction in power grid consumption highlights the potential for significant energy savings.

From a percentage standpoint, as the electrolyser power increases, the power grid consumption decreases sensibly by 22%, while the hydrogen storage volume increases by a substantial 182%. This implies that increasing the power of the electrolyser may not be the most prudent choice in this context, as it would require a considerably larger hydrogen storage volume to achieve only a marginal reduction in power purchased from the grid.

Some other factors can be identified as reasons to disapprove this solution. This process is inefficient due to the sum of the losses in both energy conversion processes since the efficiency of the electrolyser and the fuel cell is about 60% for both technologies, and the hydrogen compressor, if needed, compromises a lost of 10% of the power. Another factor is the economic perspective
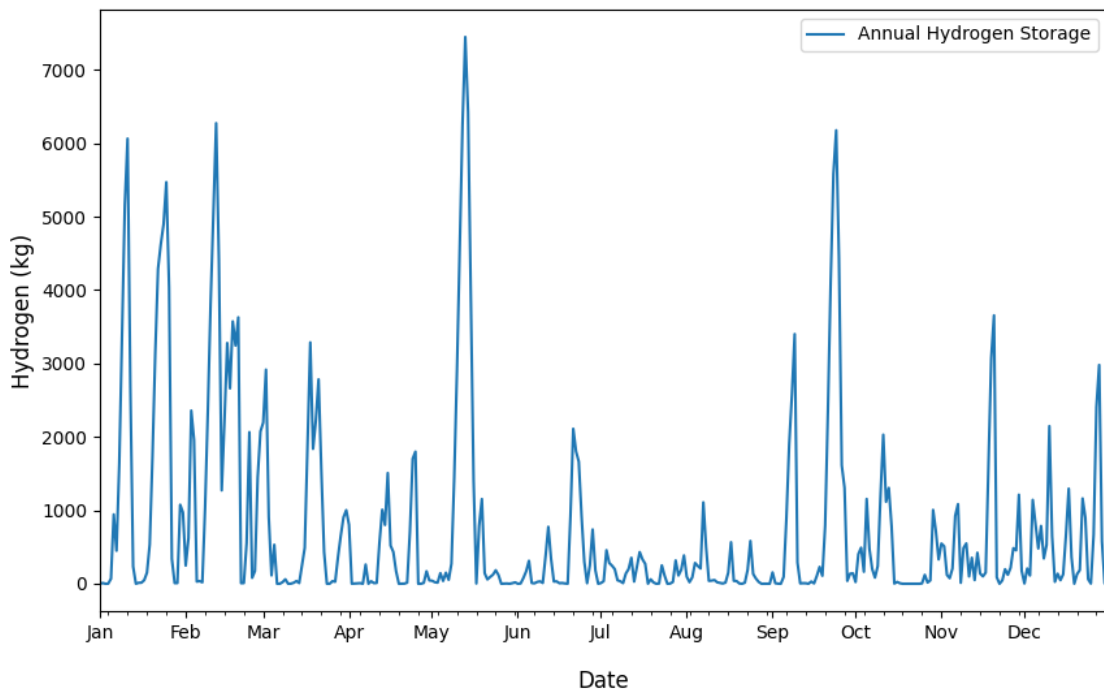
Figure 4.8: Annual quantity of the hydrogen in the HST with the integration of an electrolyser with 4000 kW.

of this system, since both the electrolyser and the fuel cell are expensive technological devices, and the HST can also be costly, especially when considering the need for a storage volume of this magnitude. Thus purchasing electricity from the grid to meet the demand might also be a more viable option, however this model option was chosen to provide a more academic and engineering-oriented analysis, since economical aspects have not been included in the initial assessment of this specific case. At this point, the feasibility of implementing this solution appears to be non-existent. However, in the future, if technology prices continue to follow the current trend and improve in terms of performance, there is a possibility that this solution could become viable and reach a point where it becomes an optimized and economically attractive choice.

Additionally, such a large storage volume would occupy a significant amount of space, making it impractical in many real-world scenarios. Figure 4.8 illustrates the annual quantity of hydrogen in the HST for an example of integration of an electrolyser with a 4000 kW capacity. This graph reveals that the tank storing the hydrogen will only reach its full capacity during specific periods of the year. There are notable peaks in the graph, especially outside of the summer season, with a significant peak occurring in the middle of May and June. This behavior results in an oscillating tank's capacity which, in most instances, will not be at full capacity, potentially leading to inefficient use of storage space.

There are several approaches that can be explored to enhance the overall model. For instance, implementing a maximum capacity for the HST could help reduce costs and space requirements. In this setup, when the HST reaches its maximum capacity, any excess hydrogen could be redi-

rected into a pipeline for storage or other uses. However, this approach might lead to an increase in power purchases from the grid, since it represents a trade-off but can represent an improvement in both cost-effectiveness and system performance by efficiently managing hydrogen storage capacity.

4.5   Case 2 - Economical evaluation of a hydrogen production system

In the previous case, a fuel cell was used to compensate for the energy demanded when the wind farm couldn't generate enough power. However, this approach was not economically viable. Thus, instead of using a fuel cell to meet the power demand, the use of the fuel cell is be neglected and the objective will be only to produce hydrogen. The aim of the study conducted is to understand the investment payback period for a model where different sizes of electrolyser units are studied across a range of hydrogen selling prices by analyzing how changes in the selling price of hydrogen impact the Return on Investment (ROI) and to evaluate the influence of the electrolyser size on this aspect.

ROI is introduced as a metric to assess the efficiency of the investment and is calculated by dividing the average annual profit or net cash inflow by the initial investment. A negative ROI or lower ROI compared to other alternatives implies that the investment may not be favorable or efficient.[35]

In the article developed by Spazzafumo et al.[51] an economic assessment of hydrogen production is carried out, and several formulas related to the initial investment are introduced. From the analysis of this paper and its application to the model in question, it can be deduced that the formula responsible for calculating the initial investment is as follows:

$$\text{Investment} = C_{\text{EL}} + C_{\text{HST}} + \sum_{i=1}^{n} \frac{C_{OM}^{\text{EL}} + C_{OM}^{\text{HST}}}{(1+d)^n} \tag{4.3}$$

Where C_{EL} represents the cost of the electrolyser, C_{HST} is the cost of the HST and respective hydrogen compression, C_{OM} is the operation and maintenance (OM) cost of electrolysis system and the HST, n is the expected lifetime of the investment and d is the interest rate. The eletrolyser used in this model, is an AEL, since the electrolyser's cost its an important parameter for the objective function. The study focuses on the profitability of hydrogen production for the wind farm. Therefore, it was assumed that the capital costs of the wind farm itself are not included in the initial investment. Additionally, the costs associated with the transportation of hydrogen were shifted to the customer, and these logistics and expenses were not considered as part of the initial investment.

Table 4.2 provides information on the economic parameters used to calculate the initial investment. It's important to note that the costs of the electrolyser, HST, and OM vary with the electrolyser's power capacity and hydrogen mass. This implies that increasing the electrolyser's specific power capacity will result in a higher total investment. The interest rate is also a parameter that has influences in the outcome of this expression, as a higher interest rate means that future

Parameter	Value
Electrolyser cost, (€/kW)[12]	967
HST cost, (€/kg)[66]	400
OM electrolyser costs, (€/kW year)[1]	20
OM HST costs, (€/kg year)[1]	30
Lifetime, years[1]	20
Interest rate, %[51]	5

Table 4.2: Economic data relatively to the investment parameters.

costs are considered less significant in today's terms, whereas a lower interest rate gives relatively more weight to future costs in today's calculations.

The power output considered in this case study remains the same as the previous case since the wind farm is common for both cases. However, the objective of this model is to directly redirect all the energy generated by the wind farm towards the electrolyser to produce hydrogen. In this configuration, a consistent volume of hydrogen is sold, and this volume is influenced by the electrolyser's capacity to produce hydrogen. The electrolyser's ability to produce hydrogen is, in turn, influenced by its maximum power capacity and the power that is redirected to it. This volume is contingent on the storage system's capacity, which acts as a buffer. For this configuration, a HST is utilized, and it is assumed that customers will require a relatively constant supply of hydrogen. This could involve daily truck deliveries for a fueling station or continuous pipeline deliveries for a refinery, for instance.

Under normal conditions, the objective is to channel all the power produced by the wind farm to the electrolyser for hydrogen production. However, depending on the capacity of the electrolyser, it is possible that all the power generated by the wind farm exceeds the electrolyser's maximum capacity. In such cases, a controller associated with the system can detect the status of the it, at that given time, and redirect the excess power that cannot be used due to the electrolyser being at its maximum hydrogen production capacity. This excess power is redirected and sold to the grid, minimizing the waste of energy produced and improving the annual cash flow. Ultimately, this leads into a lower ROI. This approach is also employed when the power generated does not meet the minimum power requirement of the electrolyser, and thus, this excess energy is sold to the grid, since AELs are only able to produce hydrogen when the power fed into them surpasses 15% of its maximum power consumption.

Bearing this in mind, it is now possible to assess the annual cash flow or the income that the employment of this system will deliver. Based on the conditions explained earlier, it becomes feasible to develop a formula that calculates the revenue and the income generated. For this purpose, it is essential to calculate the estimated annual hydrogen production, as well as the power sold to the grid during that year. The evaluation of this parameters will ultimately led to the equation 4.4.

$$\text{Income} = SP_{H_2} \cdot m_{H_2} + SP_{grid} \cdot P_{grid} \tag{4.4}$$

Where SP_{H_2} represents the selling price of hydrogen, m_{H_2} is the annual mass production of

hydrogen, P_{grid} is the annual power redirected to the grid and SP_{grid} is the selling price of the that power.

For each hydrogen selling price chosen, the ROI will vary because the hydrogen selling price is a variable used to calculate the annual income, which in turn affects the ROI. Therefore, in a first analysis, it is important to evaluate the behavior of the ROI with the increment of the hydrogen selling price. For that purpose, the graphic presented in figure 4.9 was created, where for each hydrogen price, the lowest ROI was chosen from an interval of electrolyser capacities ranging from 500 kW to 10000 kW. Additionally, a fixed value of 0.07 euros per kWh[3] was employed for the selling price of the power redirected to the grid, as this parameter was not the focus of the study.
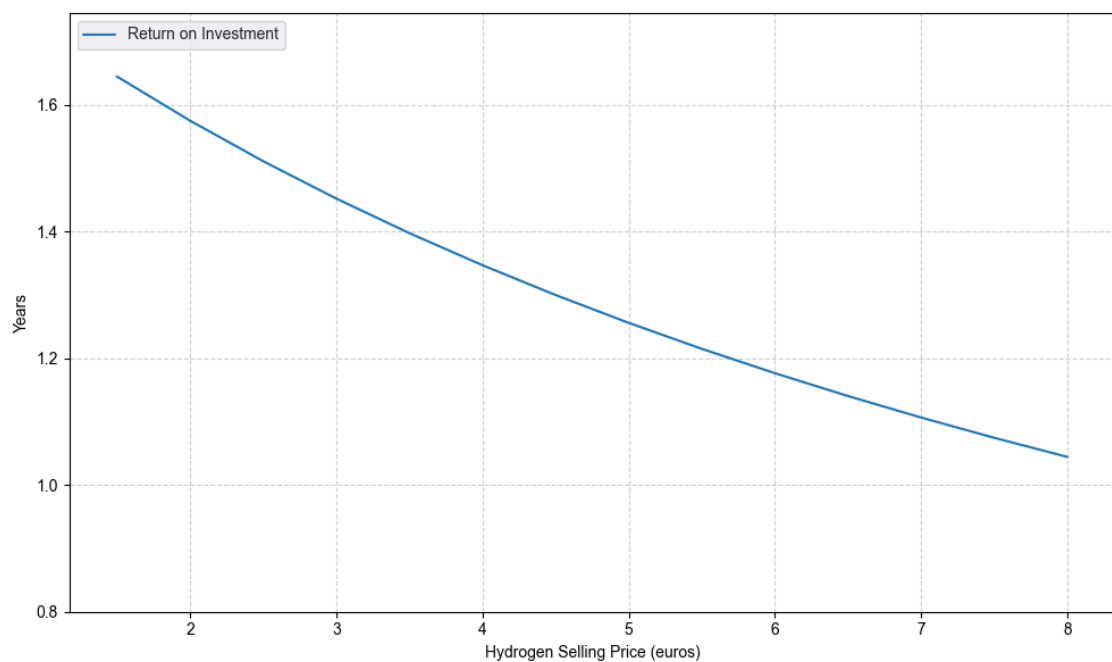

Figure 4.9: Variation of the ROI with the hydrogen selling price.

As can be deduced from Equation 4.4, an increase in the hydrogen selling price will result in higher income, reducing the number of years required to recoup the initial investment. By analyzing this graph, it becomes evident that it follows the expected trend.

To further investigate the impact of electrolyser capacity on ROI, a graph showing the dependency of ROI on electrolyser power consumption was created and it is present in figure 4.10.

For this graphic, the hydrogen selling price was fixed at five euros per kg, which is a value in the middle of the range of prices evaluated, and a not very unusual green hydrogen price. It is evident that this graphic is represented by an ascending curve, indicating that electrolysers with lower capacity will result in a lower ROI. Based on this observation, a deeper analysis of this case should also focus on evaluating the behavior of annual income and investment with the increment in electrolyser power capacity.
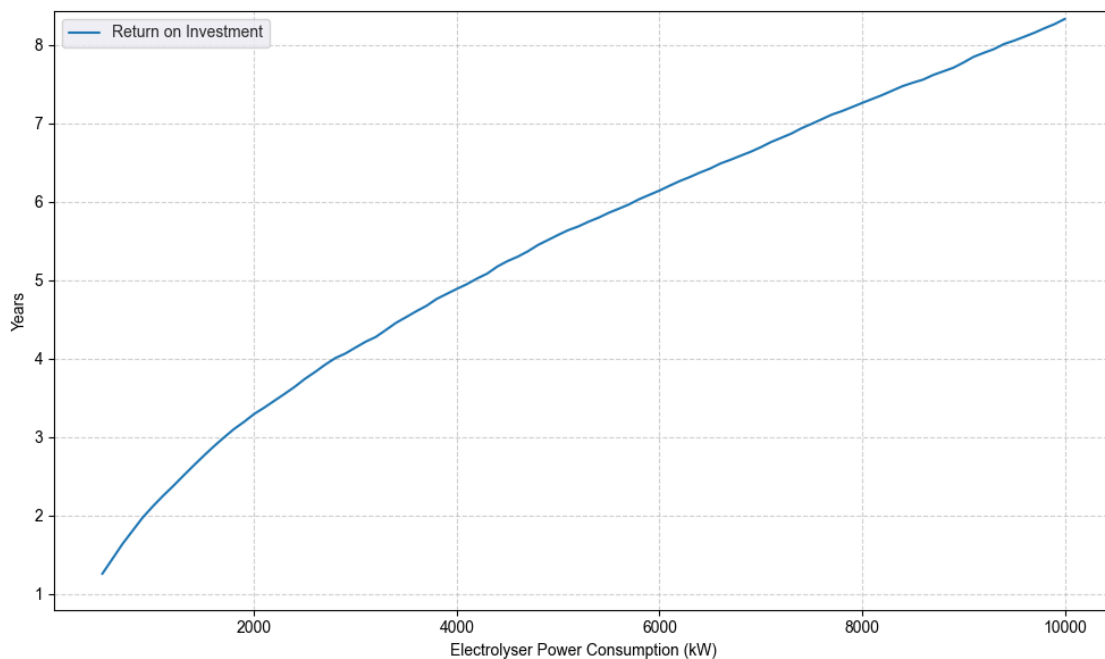
Figure 4.10: ROI of the system with fixed hydrogen selling price.

In order to conduct the analysis mentioned earlier, figure 4.11 illustrates how annual income correlates with the investment allocated to this hydrogen production technology. It's evident that both variables increase as the power capacity of the electrolyser grows, primarily because higher capacity results in a greater hydrogen production. Conversely, the investment follows an almost linear pattern since it's primarily determined by fixed costs associated with the electrolyser and HST. These costs are contingent solely on their respective capacities since there CAPEX was previously defined. Thus, by despising the influence of OM costs, since the investment in this parameter is much lower when compared to the other costs, the total investment can be described as linear, with the impact of the interest rate over the years deviating from this linear pattern.

However, the variation in investment, with the increment in electrolyser's power capacity, significantly surpasses the one which occurs with annual income. Investment increases by approximately 15 million euros across the entire range of electrolyser capacities studied, whereas annual income fluctuates only modestly, ranging from 0.6 to 1.9 million euros. This phenomenon provides insight into the ROI trends depicted in Figure 4.10.

Based on this analysis, it can be concluded that, from a financial return perspective, that higher electrolyser capacity will lead to increased investment costs, thereby reducing ROI. However, this doesn't necessarily imply that implementing an electrolyser with lower capacity is the best choice in this scenario. After achieving ROI, all income becomes profit. Therefore, the optimal capacity depends on the investor's strategy, understanding which capacity is more suitable for the wind farm, the level of investment they are willing to make, and which option will ultimately yield higher profits.

With the aim of analysing this situation, the profit that would be obtained by implementing
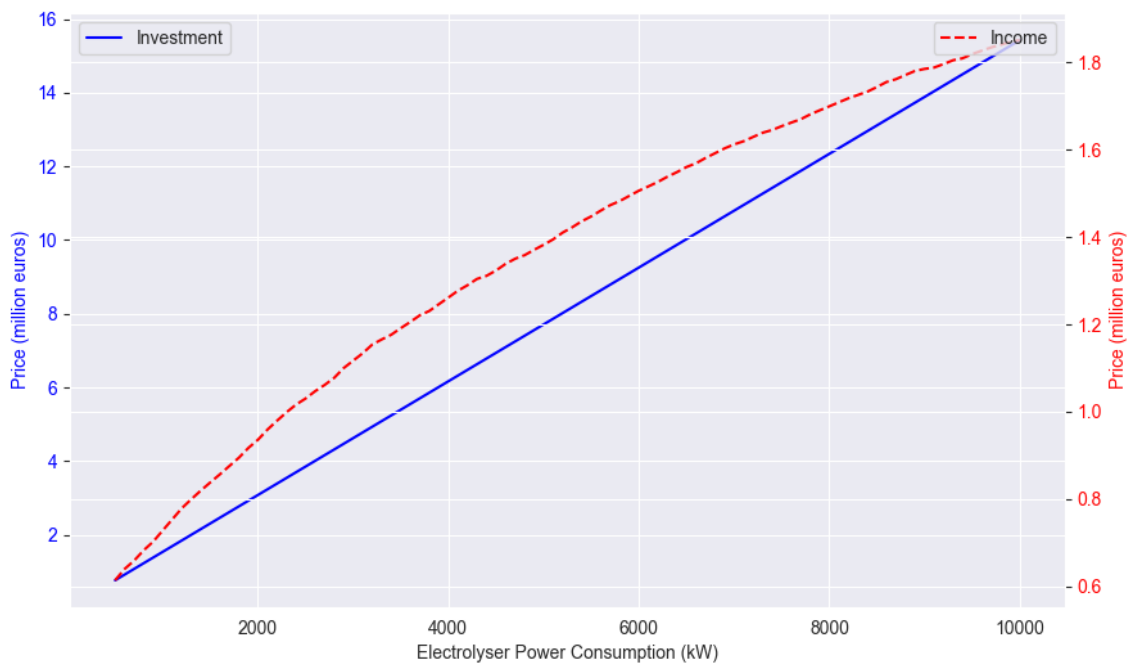
Figure 4.11: Variation of the investment and income of the system with fixed hydrogen selling price.

this solution was calculated and displayed in figure 4.12. It was assumed that this profit would be calculated over the predicted lifetime of the system, which is twenty years. Additionally, it was considered that the income would remain constant each year, resulting in a total income over this period equal to twenty times the annual income. Therefore, the profit at this point is calculated by subtracting the total income by the investment made in acquiring the electrolyser and the HST, along with the OM costs, over these twenty years.

From the analysis of this graphic, it is evident that there is a general increase in profit with the electrolyser power capacity. However, it's important to note that higher electrolyser power capacity leads to a longer time to recoup the initial investment, as it takes more time to achieve ROI. Nevertheless, once ROI is achieved under these conditions, as the income afterwards becomes pure profit it will lead into higher income after this period. Ultimately, the profit reaches its peak at 21.88 million euros when using an electrolyser with a capacity of 8,900 kW. This would entail a fixed investment of 13.73 million euros and an HST capacity of 1,908 Nm^3, capable of storing 169.81 kg of compressed hydrogen.

However, this maximum profit is relative to a study with a fixed hydrogen selling price of five euros. By applying the same method to the range studied before in figure 4.9, it's possible to determine which electrolyser's power capacity would result in higher profits over twenty years for a given hydrogen selling price. When the hydrogen selling price increases, the investment remains unchanged, since the changes only occur in the annual income received given that the annual income is highly dependent on the hydrogen selling price, therefore an increase of this price will ultimately lead to higher profits.
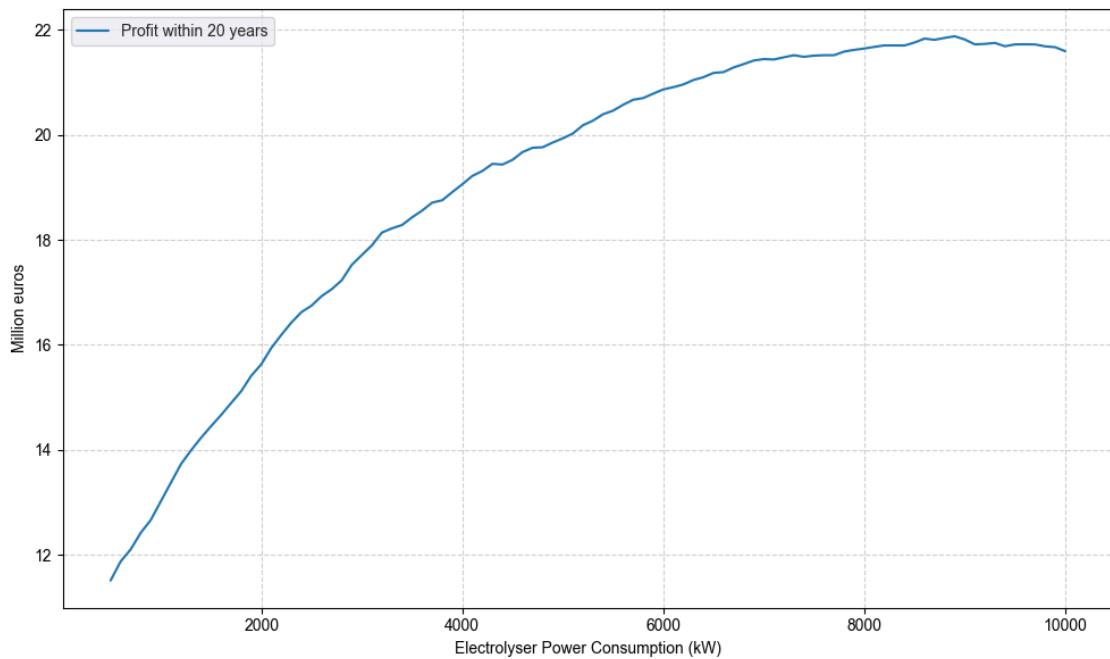
Figure 4.12: Variation of the profit in twenty years with the electrolyser power, for fixed hydrogen selling price.

This case provides an optimistic analysis of the electrolysis scenario. It is important to acknowledge that the actual outcomes may vary, as it is not realistic to assume that the regulatory power market will accept every bid from this electrolysis facility, since the hydrogen selling price is influenced by market dynamics and customer demand for hydrogen. Therefore, a more extensive analysis would be needed to determine a feasible range of hydrogen selling prices that would attract customers. Once that range is established, a study similar to the one presented in figure 4.12 could be conducted to identify the optimal electrolyser size for maximizing profits over twenty years.

Chapter 5

Conclusions and Future Works

This thesis has undertaken a exploration into the utilization of wind energy for hydrogen production passing through its application as an efficient energy storage medium and also its economic viability. This study began with a comprehensive examination of wind energy, highlighting its status on both a global scale and within the context of Portugal and the complexities behind wind energy generation, including the specification of various factors that play a crucial role in understanding the dynamics of this renewable energy source.

Subsequently, the focus shifted to hydrogen as promising energy carrier with multifaceted potential applications. The thesis delved into the fundamental properties of hydrogen and provided an extensive overview of the technologies used in its production, encompassing various electrolyser and fuel cell technologies.

A significant contribution of this thesis lies in its comprehensive analysis of mathematical models and analytical methodologies encompassing all components involved in the conversion of wind kinetic energy into hydrogen and its reconversion into electrical energy. These theoretical foundations allowed to estimate the power production at a hypothetical wind farm from the wind speed at that particular site during a year, and for the implementation of two practical case studies, serving as demonstrations of the earlier explored theoretical concepts.

The first case study investigated the feasibility of utilizing hydrogen as an energy storage medium in wind energy systems. It addressed the entire process, from wind energy generation to hydrogen production and subsequent conversion back into power through fuel cells. This analysis provided valuable insights into the practicality of such systems and their potential role in addressing energy storage challenges.

The use of hydrogen, along with electrolyser and fuel cell technologies, is still relatively uncommon worldwide, although these technologies are experiencing consistent growth. Looking to the future, there is potential for continuous advancements that could lead to more cost-effective and high-performing devices. As these technologies continue to mature and become more widely adopted, they have the potential to play a crucial role in addressing energy storage and sustainability challenges. The ongoing development and adoption of hydrogen-based systems hold promise for a cleaner and more sustainable energy future.

The second case study shifted the focus to economic considerations, exploring the financial dynamics of a hydrogen generation system. It delved into factors such as return on investment, profit generation, and the influence of variables like hydrogen selling prices and electrolyser capacities on financial outcomes. This analysis provided valuable insights into the economic viability of hydrogen production within the context of wind energy. ROI emerged as a critical parameter, indicating that the selling price of hydrogen significantly influences the profitability and payback period of wind-to-hydrogen systems. Higher hydrogen prices can expedite the return on investment.

Additionally, this case also offered a solution to maximize profits over the system's lifetime by selecting the optimal electrolyser size for a fixed hydrogen selling price, these systems can become more economically appealing. This approach ensures that the investment made in such systems obtains the highest possible returns, further enhancing their economic viability.

In summary, this thesis has provided a comprehensive overview of the integration of wind energy and hydrogen production, spanning from theoretical foundations to practical applications and economic considerations. By harnessing wind energy for hydrogen production, these systems hold great potential to contribute to a sustainable and cleaner energy since wind and hydrogen are aligned with the 2030 plans of increasing the share of renewable energies worldwide. As technology continues to advance and global efforts intensify, we can expect wind and hydrogen to play pivotal roles in achieving a more sustainable and greener energy landscape by 2030 and beyond. Hence, as the costs of this technology continue to decrease while performance improves, it is anticipated that an increasing number of investors will be drawn to this type of energy solution. Over time, it is expected to become a more economically attractive choice, further supporting its adoption and contributing to the transition toward cleaner and more sustainable energy systems. Their success will also depend on a careful comprehension of technical, economic, and environmental considerations, as well as on continual technological improvements. Ultimately, the path to a greener future calls for careful planning, creativity, and cooperation.

5.1 Future Works

Regarding future works, to improve the knowledge of the complex dynamics at work in power markets, the investigation might also use more sophisticated optimization approaches, such as Nonlinear Optimization or even Machine Learning techniques that can lead into more refined strategies to maximize the profit.

Another case that could be evaluated focuses on improving and expanding the operational strategy of energy systems in the setting of electricity markets distinguished by variable costs and uncertainty. Using techniques such as price arbitrage, in which surplus energy is strategically held during periods of low electricity costs and sold when prices rise, it is possible to optimize the wind farm's potential for profit. This strategy becomes even more crucial when you consider how the wind farm can impact how much local electricity costs.

In conclusion, there is a lot of promise in this field's future initiatives. There is potential for even larger improvements in the combination of wind energy and hydrogen production leading a step towards a more sustainable energy future with the use of operational tactics and investigating optimization approaches. The following of these approaches will aid to create a future energy paradigm that is cleaner and more effective.

References

[1] An economic analysis of the production of hydrogen from wind-generated electricity for use in transport applications. `https://shs.hal.science/halshs-00582762`. [Accessed 08-07-2023].

[2] Comparing Fuel Cell Technologies - GenCell - Fuel Cell Generators. `https://www.gencellenergy.com/news/comparing-fuel-cell-technologies/`. [Accessed 02-Jun-2023].

[3] EZU Energia — ezu.pt. `https://ezu.pt/venda_de_excedente`.

[4] How Do Wind Turbines Work. `https://www.energy.gov/eere/wind/how-do-wind-turbines-work`.

[5] Hydrogen forecast DNV — dnv.com. `https://www.dnv.com/Publications/hydrogen-forecast-226443`. [Accessed 31-Mar-2023].

[6] MERRA-2 — gmao.gsfc.nasa.gov. `https://gmao.gsfc.nasa.gov/reanalysis/MERRA-2/`. [Accessed 24-May-2023].

[7] Plano Nacional de Energia e Clima (PNEC). `https://www.apambiente.pt/clima/plano-nacional-de-energia-e-clima-pnec`.

[8] Renewables 2022 – Analysis - IEA. `https://www.iea.org/reports/renewables-2022/`.

[9] Wind turbine - Energy Education. `https://energyeducation.ca/encyclopedia/Wind_turbine`.

[10] World Energy Outlook 2022 – Analysis - IEA. `https://www.iea.org/reports/world-energy-outlook-2022/executive-summary`.

[11] EÓLICA DA ARADA, S.A. ESTUDO DE IMPACTE AMBIENTAL PARQUE EÓLICO DE ARADA/MONTEMURO VOLUME 2 – RESUMO NÃO TÉCNICO T366.1.2. Technical report, AP Ambiente, 2021.

[12] Argus hydrogen and future fuels. `https://www.argusmedia.com/-/media/Files/methodology/argus-hydrogen-and-future-fuels.ashx`, 2023. [Accessed 08-07-2023].

[13] Wind energy in Europe: 2022 Statistics and the outlook for 2023-2027. `https://windeurope.org/intelligence-platform/product/wind-energy-in-europe-2022-statistics-and-the-outlook-for-2023-2027/`, february 2023.

[14] H. R. V. . N. . M. 2014. Special issue "hitachi technology 2014". `https://www.hitachi.com/rev/pdf/2014/r2014_technology_all.pdf`. [Accessed 31-Mar-2023].

[15] T. Agarwal, S. Verma, and A. Gaurh. Issues and challenges of wind energy. In *2016 International Conference on Electrical, Electronics, and Optimization Techniques (ICEEOT)*. IEEE, Mar. 2016.

[16] K. Almutairi, S. S. Hosseini Dehshiri, S. J. Hosseini Dehshiri, A. Mostafaeipour, M. Jahangiri, and K. Techato. Technical, economic, carbon footprint assessment, and prioritizing stations for hydrogen production using wind energy: A case study. *Energy Strat. Rev.*, 36(100684):100684, July 2021.

[17] A. Arshad, H. M. Ali, A. Habib, M. A. Bashir, M. Jabbal, and Y. Yan. Energy and exergy analysis of fuel cells: A review. *Thermal Science and Engineering Progress*, 9:308–321, Mar. 2019.

[18] D. Bairrão, J. Soares, J. Almeida, J. F. Franco, and Z. Vale. Green hydrogen and energy transition: Current state and prospects in portugal. *Energies*, 16(1):551, Jan. 2023.

[19] F. Bañuelos-Ruedas, C. Ángeles Camacho, and S. Rios-Marcuello. Methodologies used in the extrapolation of wind speed data at different heights and its impact in the wind energy resource assessment in a region. [Accessed 31-Mar-2023].

[20] R. Bhandari, C. A. Trudewind, and P. Zapp. Life cycle assessment of hydrogen production via electrolysis – a review. *Journal of Cleaner Production*, 85:151–163, Dec. 2014.

[21] K. Bosio. Technical and economic analysis of state-of-the-art electrolytic systems for hydrogen production, 2021. Rel. Massimo Santarelli, Luca Piantelli, Giulio Buffo. Politecnico di Torino, Corso di laurea magistrale in Ingegneria Energetica E Nucleare.

[22] A. Buttler and H. Spliethoff. Current status of water electrolysis for energy storage, grid balancing and sector coupling via power-to-gas and power-to-liquids: A review. *Renewable and Sustainable Energy Reviews*, 82:2440–2454, Feb. 2018.

[23] G. Calado and R. Castro. Hydrogen production from offshore wind parks: Current situation and future perspectives. *Applied Sciences*, 11(12):5561, June 2021.

[24] M. Cerchio, F. Gullí, M. Repetto, and A. Sanfilippo. Hybrid energy network management: Simulation and optimisation of large scale PV coupled with hydrogen generation. *Electronics*, 9(10):1734, Oct. 2020.

[25] A. Claro, J. A. Santos, and D. Carvalho. Assessing the future wind energy potential in portugal using a CMIP6 model ensemble and WRF high-resolution simulations. *Energies*, 16(2):661, Jan. 2023.

[26] M. El-Shafie, S. Kambara, and Y. Hayakawa. Hydrogen production technologies overview. *Journal of Power and Energy Engineering*, 07(01):107–154, 2019.

[27] J. L. Holechek, H. M. E. Geli, M. N. Sawalhah, and R. Valdez. A global assessment: Can renewable energy replace fossil fuels by 2050? *Sustainability*, 14(8):4792, Apr. 2022.

[28] INEGI and APREN. Wind Farms in Portugal. `https://e2p.inegi.up.pt/reports/parks/portugal_parques_eolicos_2022.pdf`.

[29] G. Kakoulaki, I. Kougias, N. Taylor, F. Dolci, J. Moya, and A. Jäger-Waldau. Green hydrogen in europe – a regional assessment: Substituting existing production with electrolysis powered by renewables. *Energy Conversion and Management*, 228:113649, Jan. 2021.

[30] M. Kamran and M. R. Fazal. *Renewable energy conversion systems*. Academic Press, San Diego, CA, May 2021.

[31] R. Karki and R. Billinton. Cost-effective wind energy utilization for reliable power supply. *IEEE Transactions on Energy Conversion*, 19(2):435–440, June 2004.

[32] A. Khalilnejad and G. Riahy. A hybrid wind-PV system performance investigation for the purpose of maximum hydrogen production and storage using advanced alkaline electrolyzer. *Energy Conversion and Management*, 80:398–406, Apr. 2014.

[33] Y. Kumar, J. Ringenberg, S. S. Depuru, V. K. Devabhaktuni, J. W. Lee, E. Nikolaidis, B. Andersen, and A. Afjeh. Wind energy: Trends and enabling technologies. *Renewable and Sustainable Energy Reviews*, 53:209–224, Jan. 2016.

[34] T. M. Letcher. *Wind energy engineering*. Academic Press, San Diego, CA, May 2017.

[35] H. T. LUK, H. M. LEI, W. Y. NG, Y. JU, and K. F. LAM. Techno-economic analysis of distributed hydrogen production from natural gas. *Chinese Journal of Chemical Engineering*, 20(3):489–496, June 2012.

[36] J. F. Manwell, J. G. McGowan, and A. L. Rogers. *Wind energy explained*. Wiley-Blackwell, Hoboken, NJ, 2 edition, Dec. 2009.

[37] M. M. Mark Ruth, Ahmad Mayyas. Manufacturing competitiveness analysis for pem and alkaline water electrolysis systems, 2017. [Accessed 31-Mar-2023].

[38] P. P. A. C. S. P. C. B. S. C. N. C. Y. G. L. G. M. Masson-Delmotte, V.; Zhai. *PCC Climate Change 2021: The Physical Science Basis*. Cambridge University Press: Cambridge, UK, Fourth edition, 2021.

[39] M. Mohsin, A. Rasheed, and R. Saidur. Economic viability and production capacity of wind generated renewable hydrogen. *International Journal of Hydrogen Energy*, 43(5):2621–2630, Feb. 2018.

[40] A. Mostafaeipour, M. Khayyami, A. Sedaghat, K. Mohammadi, S. Shamshirband, M.-A. Sehati, and E. Gorakifard. Evaluating the wind energy potential for hydrogen production: A case study. *International Journal of Hydrogen Energy*, 41(15):6200–6210, Apr. 2016.

[41] K. Murthy and O. Rahi. A comprehensive review of wind resource assessment. *Renewable and Sustainable Energy Reviews*, 72:1320–1342, May 2017.

[42] D. Nelson, M. Nehrir, and C. Wang. Unit sizing and cost analysis of stand-alone hybrid wind/PV/fuel cell power generation systems. *Renewable Energy*, 31(10):1641–1656, Aug. 2006.

[43] N. R. E. L. (NREL). Nrel - wind-to-hydrogen project. https://www.nrel.gov/hydrogen/wind-to-hydrogen.html. [Accessed 24-May-2023].

[44] U. D. of Energy Fuel Cell Technologies Office. Fuel cells, 2015. https://www.energy.gov/eere/fuelcells/articles/fuel-cells-fact-sheet.

[45] A. Peña, P.-E. Réthoré, and M. P. Laan. On the application of the jensen wake model using a turbulence-dependent wake decay coefficient: the sexbierum case. *Wind Energy*, 19(4):763–776, May 2015.

[46] M. Rezaei, N. Naghdi-Khozani, and N. Jafari. Wind energy utilization for hydrogen production in an underdeveloped country: An economic investigation. *Renewable Energy*, 147:1044–1057, Mar. 2020.

[47] R. Saidur, N. Rahim, M. Islam, and K. Solangi. Environmental impact of wind energy. *Renewable and Sustainable Energy Reviews*, 15(5):2423–2430, June 2011.

[48] A. P. Schaffarczyk. Aerodynamics and aeroelastics of wind turbines. In *Wind Power Generation and Wind Turbine Design*, pages 89–120. WIT Press, June 2010.

[49] R. Shakoor, M. Y. Hassan, A. Raheem, and Y.-K. Wu. Wake effect modeling: A review of wind farm layout optimization using jensens model. *Renewable and Sustainable Energy Reviews*, 58:1048–1059, May 2016.

[50] S. Shamshirband, K. Mohammadi, C. W. Tong, D. Petković, E. Porcu, A. Mostafaeipour, S. Ch, and A. Sedaghat. RETRACTED ARTICLE: Application of extreme learning machine for estimation of wind speed distribution. *Climate Dynamics*, 46(5-6):1893–1907, June 2015.

[51] G. Spazzafumo and G. Raimondi. Economic assessment of hydrogen production in a renewable energy community in italy. *e-Prime - Advances in Electrical Engineering, Electronics and Energy*, 4:100131, June 2023.

[52] P. Stackhouse. NASA POWER | Docs | Methodology | Data Sources - NASA POWER | Docs — power.larc.nasa.gov. https://power.larc.nasa.gov/docs/methodology/data/sources/. [Accessed 24-May-2023].

[53] H. Sun, X. Gao, and H. Yang. A review of full-scale wind-field measurements of the wind-turbine wake effect and a measurement of the wake-interaction effect. *Renewable and Sustainable Energy Reviews*, 132:110042, Oct. 2020.

[54] T. W. D. Team. Windpowerlib documentation. https://windpowerlib.readthedocs.io/_/downloads/en/latest/pdf/, 2023.

[55] W. Tong. Fundamentals of wind energy. In *Wind Power Generation and Wind Turbine Design*, pages 3–48. WIT Press, June 2010.

[56] A. Ursua, L. M. Gandia, and P. Sanchis. Hydrogen production from water electrolysis: Current status and future trends. *Proceedings of the IEEE*, 100(2):410–426, Feb. 2012.

[57] I. Vincent and D. Bessarabov. Low cost hydrogen production by anion exchange membrane electrolysis: A review. *Renewable and Sustainable Energy Reviews*, 81:1690–1704, Jan. 2018.

[58] J. Walkowiak-Kulikowska, J. Wolska, and H. Koroniak. Polymers application in proton exchange membranes for fuel cells (PEMFCs). *Physical Sciences Reviews*, 2(8), July 2017.

[59] E. Weidner, R. Ortiz Cebolla, and J. Davies. Global deployment of large capacity stationary fuel cells–drivers of, and barriers to, stationary fuel cell deployment. EUR JRC115923, Publications Office of the European Union, Luxembourg, 2019.

[60] V. Yaramasu and B. Wu. *Model predictive control of wind energy conversion systems*. IEEE Press Series on Power Engineering. John Wiley & Sons, Nashville, TN, Jan. 2017.

[61] B. Yodwong, D. Guilbert, M. Phattanasak, W. Kaewmanee, M. Hinaje, and G. Vitale. AC-DC converters for electrolyzer applications: State of the art and future challenges. *Electronics*, 9(6):912, May 2020.

[62] D. Yogi Goswami and F. Kreith, editors. *Energy Conversion*. Mechanical and Aerospace Engineering Series. CRC Press, Boca Raton, FL, 2 edition, June 2017.

[63] M. Yue, H. Lambert, E. Pahon, R. Roche, S. Jemei, and D. Hissel. Hydrogen energy systems: A critical review of technologies, applications, trends and challenges. *Renewable and Sustainable Energy Reviews*, 146:111180, Aug. 2021.

[64] A. Zbiciak and T. Markiewicz. A new extraordinary means of appeal in the polish criminal procedure: the basic principles of a fair trial and a complaint against a cassatory judgment. *Access to Justice in Eastern Europe*, 6(2):1–18, Mar. 2023.

[65] F. Zhang, P. Zhao, M. Niu, and J. Maddy. The survey of key technologies in hydrogen energy storage. *Int. J. Hydrogen Energy*, 41(33):14535–14552, Sept. 2016.

[66] Y. Zhang, A. Lundblad, P. E. Campana, and J. Yan. Comparative study of battery storage and hydrogen storage to increase photovoltaic self-sufficiency in a residential building of sweden. *Energy Procedia*, 103:268–273, Dec. 2016.